

**A Design Study for Multivariable Feedback Control  
For a Variable Speed Wind Turbine**

دراسة مقارنة في تصميم نظم التحكم ذات المتغيرات المتعددة لمحركات الرياح  
متغيرة السرعة

by

**MELAD BAHJAT ABDELAZIZ AL AQRA**

**A dissertation submitted in fulfilment  
of the requirements for the degree of  
MSc SYSTEMS ENGINEERING**

at

**The British University in Dubai**

**Professor Robert Whalley**

**October 2017**

---

## DECLARATION

I warrant that the content of this research is the direct result of my own work and that any use made in it of published or unpublished copyright material falls within the limits permitted by international copyright conventions.

I understand that a copy of my research will be deposited in the University Library for permanent retention.

I hereby agree that the material mentioned above for which I am author and copyright holder may be copied and distributed by The British University in Dubai for the purposes of research, private study or education and that The British University in Dubai may recover from purchasers the costs incurred in such copying and distribution, where appropriate.

I understand that The British University in Dubai may make a digital copy available in the institutional repository.

I understand that I may apply to the University to retain the right to withhold or to restrict access to my thesis for a period which shall not normally exceed four calendar years from the congregation at which the degree is conferred, the length of the period to be specified in the application, together with the precise reasons for making that application.

A handwritten signature in black ink, consisting of a stylized, cursive script that begins with a large, rounded 'M' and ends with a long, horizontal tail stroke.

Melad Al Aqra

## **COPYRIGHT AND INFORMATION TO USERS**

The author whose copyright is declared on the title page of the work has granted to the British University in Dubai the right to lend his/her research work to users of its library and to make partial or single copies for educational and research use.

The author has also granted permission to the University to keep or make a digital copy for similar use and for the purpose of preservation of the work digitally.

Multiple copying of this work for scholarly purposes may be granted by either the author, the Registrar or the Dean of Education only.

Copying for financial gain shall only be allowed with the author's express permission.

Any use of this work in whole or in part shall respect the moral rights of the author to be acknowledged and to reflect in good faith and without detriment the meaning of the content, and the original authorship.

## Abstract

Electrical energy consumption is dramatically increasing due to industry developments and expanding of urban areas. Fossil fuels as an energy resource has many environmental and human health effects. Consequently, the demand for utilizing renewable clean energy arises. Wind energy is a significant source of energy since it is clean, renewable, and cost effective in comparison with other renewable resources like photovoltaic which has higher costs in production and maintenance. This research work deals with variable speed pitch controlled wind turbine and covers the modelling of wind turbines as an aerodynamic, mechanical and electrical system. The preliminary history of feedback control will be reviewed along with background of wind turbine developments. Moreover, the mathematical modelling of a Variable Speed Wind Turbine VSWT will be presented. This study is based on evaluating the performance and energy consumption of two controllers. The first controller is the new Least Effort controller which proved to have superior optimization of the consumed energy by the controller with a simple design using only proportional feedback. The other method is H-infinity controller with mixed sensitivity criteria. This controller results in a fast response but with heavy in energy consumptions and controller complexity. A comparison between the two control techniques showing the simulation results will be provided.

## خلاصة البحث

مع الازدياد الكبير في استهلاك الطاقة الكهربائية بسبب التوسع في الصناعات وفي استغلال المناطق الحضرية، ومع التأثير السبيء لاستخدام الوقود الأحفوري على البيئة والإنسان كان لزاما علينا استخدام الطاقة البديلة المتجددة. هناك العديد من أنواع الطاقة المتجددة ولكن تم اختيار طاقة الرياح وذلك لانخفاض تكاليف صناعتها وصيانتها عن التقنيات الأخرى كالطاقة الشمسية. يستعرض هذا البحث في البداية محرك طاقة الرياح المتغير السرعة من حيث بداية استخدامه وكيفية تصميمه من الناحية الهوائية والكهربائية والميكانيكية، وبعد ذلك يتم الحديث عن تاريخ نظرية التحكم التقليدية. ثم يتم استعراض كفاءة طريقتين للتحكم بمحركات طاقة الرياح، أحدهما طريقة جديدة تقوم على أساس استهلاك أقل طاقة ممكنة للتحكم. أما الطريقة الأخرى فهي طريقة كلاسيكية تصمم على أساس أخذ بعين الإعتبار أي تأثيرات يتعرض لها النظام. يختم البحث بمقارنة بين الطريقتين من أكثر من ناحية ولكن مع التأكيد على أن التقنية الجديدة هي المفضلة في مجال محرك طاقة الرياح وذلك لبساطتها وقلة استهلاكها للطاقة بشكل أقل بكثير عن التقنية الأخرى.

## **Acknowledgements:**

I would first like to thank my supervisor Professor Robert Whalley. The door to Professor Whalley office was always open whenever support was needed and He steered me in the right direction whenever I needed.

I would also like to thank Dr. Alaa Ameer who supported and guided me during my master study.

Without their participation and input, the dissertation could not have been successfully conducted.

## **Dedication:**

To my mother, "Weak without your daily prayers, I can no longer stand"

To my Father for his advises and support,

To my brothers and Sisters,

To my wife, " To whom I Owe the Leaping Delight",

To my Son, Yahya and my two roses Taima and Sarah,

To all my people in Jordan and Palestine,

To my second home The UAE.

I dedicate my work to you.

# Table of Contents:

Table of Contents: .....	I
List of Figures: .....	III
Notations:.....	V
Chapter I .....	1
1. Introduction .....	1
1.1. Research Background .....	1
1.2. Problem Statement .....	8
1.3. Research Objectives: .....	9
1.4. Research Organization .....	10
Chapter II .....	11
2. Literature Review .....	11
2.1. Automatic Control .....	11
2.2. Wind Turbine .....	17
2.2.1. Wind Turbine Control .....	19
2.2.2. Wind Turbine Dynamics .....	25
2.3. Least Effort Regulation. .....	29
2.4. H-infinity Method. .....	30
Chapter III.....	32
3. Mathematical modelling .....	32
3.1. Obtaining model Transfer Function. .....	32
3.2. Open Loop Response .....	37
3.3. Least Effort Regulation Configuration. .....	39
3.4. H-infinity Method. .....	47
Chapter IV: .....	52
4. Simulation Results and Discussions .....	52
4.1. Least Effort Regulation. .....	52
4.2. H-infinity Method. .....	70
4.3. Comparison Study. .....	76
Chapter V:.....	79
5. Conclusions and Recommendations .....	79

5.1.Conclusions	79
5.2.Recommendations:	80
5.3.References	81
Appendix.....	88

## List of Figures:

<b>Figure 1-1-1, Horizontal and Vertical Axis Wind Turbines</b>	2
<b>Figure 1-1-2, Wind Turbine Major Components</b>	3
<b>Figure 1-1-3, Wind Turbine Power Curve (Polinder, Slootweg &amp; Kling 2001)</b>	6
<b>Figure 2-1, Fan Tail (Myr 1970).</b>	13
<b>Figure 2-2, Mead's speed regulator</b>	14
<b>Figure 2-3, Stall Effect</b>	20
<b>Figure 2-4, Wind Speed Regions</b>	21
<b>Figure 2-5, General Structure of a FSWT of Danish Concept (Munteanu et al. 2008)</b>	22
<b>Figure 2-6, Direct in Line Wind Turbine System</b>	23
<b>Figure 2-7, Doubly Fed Induction Generator Wind Turbine System</b>	24
<b>Figure 2-8, Wind passing through an aperture</b>	25
<b>Figure 2-9, Aerofoil cross section</b>	27
<b>Figure 2-10, Pitch angle and relative wind</b>	28
<b>Figure 3-1, Wind Turbine System Model</b>	32
<b>Figure 3-2, Open Loop Block Diagram</b>	37
<b>Figure 3-3, Open Loop Response for a step change in the first input</b>	38
<b>Figure 3-4, Open Loop Response for a step change in the second input</b>	39
<b>Figure 3-5, Control system diagram</b>	47
<b>Figure 3-6, Reading off <math>\ G\ _{\infty}</math> from plot of largest principal gain (Maciejowski, 1996)</b>	49
<b>Figure 3-7, The <math>H_{\infty}</math> Framework.</b>	50
<b>Figure 4-1, Root Locus of equation (4-5)</b>	55
<b>Figure 4-2, Performance Index J.</b>	56

<b>Figure 4-3</b> , Closed Loop response with $f=0.5$ following a step change in $r_1$ (If)	58
<b>Figure 4-4</b> , Closed Loop response with $f=0.5$ following a step change in $r_2$ (Bref)	60
<b>Figure 4-5</b> , Closed Loop response with $f=0.7$ following a step change in $r_1$ (If)	61
<b>Figure 4-6</b> , Closed Loop response with $f=0.7$ following a step change in $r_2$ (Bref)	62
<b>Figure 4-7</b> , Closed Loop response with $f=0.8$ following a step change in $r_1$ (If)	63
<b>Figure 4-8</b> , Closed Loop response with $f=0.8$ following a step change in $r_2$ (Bref)	64
<b>Figure 4-9</b> , Closed Loop response following a step change in disturbance $d_1$	65
<b>Figure 4-10</b> , Closed Loop response following a step change in disturbance $d_2$	66
<b>Figure 4-11</b> , Pole-Zero graph of $G_{21}$	67
<b>Figure 4-12</b> , Pole-Zero graph for $G_{21}$ for many proportional gain values	68
<b>Figure 4-13</b> , Pole-Zero graph of $G_{21}$ with neglecting the zero	69
<b>Figure 4-14</b> , Closed loop response following a step change in $r_1$ (If)	72
<b>Figure 4-15</b> , Closed loop response following a step change in $r_2$ (Bref)	73
<b>Figure 4-16</b> , Closed loop response following a step change in disturbance $d_1$	73
<b>Figure 4-17</b> , Closed loop response following a step change in disturbance $d_2$	74
<b>Figure 4-18</b> , Singular values of sensitivity functions	75
<b>Figure 4-19</b> , Energy Consumption by both controllers.	78
<b>Figure A-1</b> , Least Effort Controller Simulation Model (Megdadi 2017)	88
<b>Figure A-2</b> , H-infinity controller Simulation model.	89

## Notations:

$\lambda$	Tip speed ratio
$\beta$	Blade pitch angle
$\rho_{air}$	Air density
$C_p(\lambda, \theta)$	Wind Turbine power coefficient
$C_q(\lambda, \beta)$	Wind Turbine torque coefficient
$v_w$	Wind speed
$m$	Wind mass passing through aperture
$A$	Wind Turbine blades swapped area
$P$	Kinetic power
$\omega$	Blades angular velocity
$AC$	Alternative current
$DC$	Direct current
$J_r$	Rotor inertia
$\tau_a$	Aerodynamic torque
$B_r$	Viscous friction coefficient at rotor
$N$	Gearbox gain ratio
$\tau_{hs}$	High speed shaft torque
$J_g$	Generator inertia
$B_g$	Viscous friction coefficient at generator
$\tau_{em}$	Generator magnetic field torque

$P_g$	Generator power
$E_g$	Voltage across stator
$I_f$	Field current
$\omega_g$	Generator angular speed
$R_L$	Load resistance
$X_g$	Generator reactance
$\eta_g$	Generator electrical efficiency
$\eta_m$	Generator mechanical efficiency
$A(s)$	Numerator of $G(s)$ matrix
$\Gamma(s)$	Finite time delay array
$y(s)$	Transformed output vector
$u(s)$	Transformed input
$r(s)$	Transformed reference input
$\acute{r}(s)$	Transformed inner loop reference input
$\delta(s)$	Disturbances vector
$h(s)$	Feedback path compensator
$k(s)$	Forward path function
$P$	Pre-compensator matrix
$F$	Outer loop gain matrix
$f_j$	Outer loop gain
$I_m$	Identity array

$\  \cdot \ _{\infty}$	H-infinity norm
$S(s)$	Sensitivity matrix
$S_s$	Steady state matrix
$G(0)$	Steady state transfer function value
$k \succ \prec h$	Outer product of k and h
$\langle k, h \rangle$	Inner product of k and h
$L(s)$	Left (row) factors of $G(s)$
$R(s)$	Right (column) factors of $G(s)$
$A(s)$	Non-singular matrix with rational functions
$d(s)$	Denominator of $G(s)$
$Q$	Coefficient array
$J$	Performance index
$n, n_1, n_2, \dots, n_{m-1}$	Gain ratios
$W_1, W_2, W_3$	Frequency dependent weighting matrices

# Chapter I

## 1. Introduction

### 1.1. Research Background

Harvesting wind energy has a deep in history, from sailing boats in the Nile, pumping water and grinding grain. In 1919, the first wind turbine was patented by the Danish Engineer, Povl Vinding depending on the aerodynamic principles.

Since that, Wind Energy is considered one of the fastest growing renewable energies in the world. The average produced power for the turbines are increasing dramatically every year, it reached 8 MW production ("10 big wind turbines | Windpower Monthly" 2017). In 2015, and as per (Wind Power Technology Brief 2016), the world installed capacity reached 434,856 MW of production.

At the end of 2015, the top countries in wind power production were: China with 148GW production, and United States came in second by producing 74GW, then Germany by producing 45GW, Spain and India came at the bottom of the list with production of 25GW and 23GW, respectively (Wind Power Technology Brief 2016).

The movement of air, is by Wind, which occurs due to the temperature differences on earth. Wind Turbines are converting kinetic energy of the wind into electrical energy. The wind makes the rotor spin, spinning rotor is connected to a shaft which is connected to a generator, which produces electricity by electromagnetic interaction.

It is interesting to know that, the wind power is proportional to the cube of the wind speed and on the swept area of the rotor. Thereby, doubling the wind speed means increasing the produced power eight times.

Wind Turbines can be categorized in various ways, by grid connection or islanded (standalone), by installation whether it is onshore or offshore and the Wind Turbine type whether it is horizontal or of the vertical axis type Figure 1-1-1.

**Vertical Axis Wind Turbines VAWT** do not produce large power but it is independent of the wind direction (Omnidirectional). It is given that name because the axis of rotation is vertical to the wind flow. Due to its low noise level, it is mostly suitable in the urban areas. Furthermore, the electric generator is installed on the ground level which makes the wind turbine structure lighter and easy for maintenance. In contrast, still vertical axis wind turbines produce less power and are difficult in control.

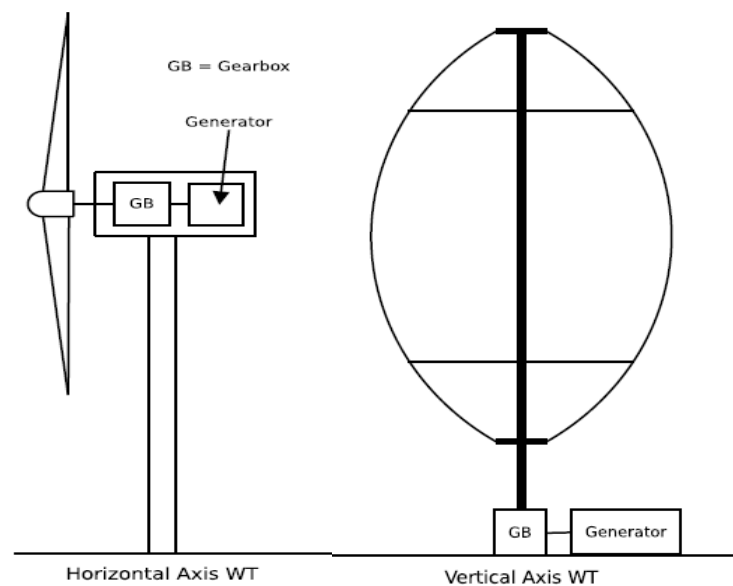


**Figure 1-1-1,** Horizontal and Vertical Axis Wind Turbines

On the other side, there is the other type of Horizontal Axis Wind Turbine HAWT.

These produce power commercially with the rotor parallel to the wind flow. This type of turbine

uses the lift force to rotate the blades which are located on the high level taking the advantage of higher speed of wind. The downside of this type is that the generator and gearbox need to be installed at a high level which means a heavier structure than vertical wind turbines. HAWTs are 40% more efficient than the VAWTs.

The basic elements of the wind turbine is the rotor which consists of blades, the hub, and the moving part which are connected to the transmission system (Gear). The gear transmits the speed from the low shaft speed which is normally between 30 to 60 rpm (Energy.gov, 2016) (connected to rotor) to the high shaft speed which is 1000 to 1800 rpm (Energy.gov, 2016) sufficient for making the generator rotates (the electrical conversion system). Moreover, the housing of the components of the wind turbine (excluding the hub and blades) is in a nacelle. In addition to that, the rotor blades, the hub and the nacelle are elevated by the tower. The diameter of the rotor determines the tower height. The following figure shows the major components of the wind turbine, Figure 1-1-2.

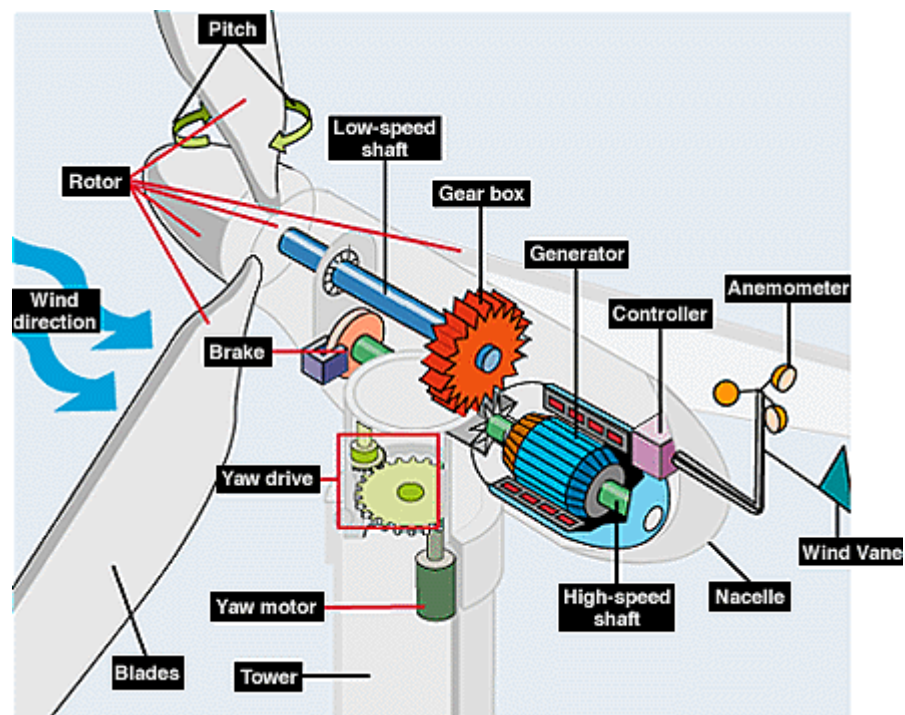


**Figure 1-1-2, Wind Turbine Major Components**

Along with that, the control system of the turbine has a significant effect on the harvested power and has three main roles:

- Controlling the rotational speed and the yaw direction.
- Collecting data during the operation such as weather conditions, vibration and electricity voltage and current.
- Communications with the system operators.

Depending on the existing power grid, it is important to install a transformer to transform the produced electricity to the required voltage and frequency, as per the grid specifications.

Generally, Wind Turbines are installed in groups which is called "Wind Farms" which have facilities such as the electrical substations, transmission cables and transformers.

The insisting challenges arising in using wind turbines are related to the optimum electrical output and the rotational speed of the rotor.

The wind power that can be harvested by a wind turbine is described by the following relation:

$$P = \frac{1}{2} \rho_{air} C_p A_r v_w^3$$

Where  $\rho_{air}$  is the air mass density in  $kg/m^3$ ,  $v_w$  is the wind speed,  $A_r$  is the swapped area by the turbine blades and  $C_p$  is the power coefficient which is different from turbine manufacturer to another depending on the design and orientation to the wind direction.

The power coefficient cannot exceed its theoretical limits which is equal to 0.593 (Betz limit). For a known wind turbine design, the power coefficient depends on two important factors which are:

- The tip speed ratio (TSR)  $\lambda$  which is equal to:  $\frac{\text{blades tip speed } (\frac{m}{s})}{\text{wind speed } (\frac{m}{s})}$
- Blade pitch angle  $\theta$  (degree) which is the angle between the blade's cord and the wind turbine plane.

Since the swept area can be expressed by an equation of a circle, so the power equation for a wind turbine with a known radius  $r$  becomes:

$$P = \frac{1}{2} \rho_{air} C_p(\lambda, \theta) \pi r^2 v_w^3$$

The value of power coefficient  $C_p$  is given by graph called power curve, which has two axes, the power coefficient and the tip speed ratio. The power curve is shown in, Figure 1-1-3.

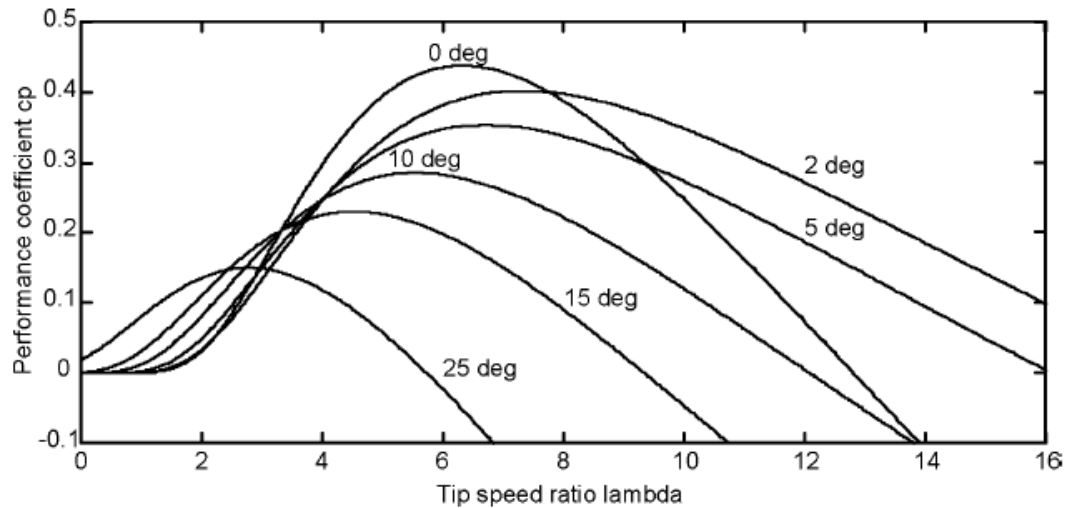


**Figure 1-1-3, Wind Turbine Power Curve (Polinder, Sloopweg & Kling 2001)**

In the power curve and by picking a pitch angle, four regions are notable and can be listed as below:

- a) Region of no power: due to low wind energy. For example, it is when the pitch angle is 15 degrees and tip speed ratio is below 2.
- b) Region of less than rated generated power: which is considered a transition region where the maintaining the aerodynamic efficiency is necessary.
- c) Region of rated generated power: in this region the aerodynamic efficiency is to be decreased to avoid the overloading that may occur to the electrical conversion system. For example, it is between tip speed ratio 4 to 6 when the pitch angle is 15 degrees, Figure 1-1-3.
- d) Region of no power: this region differs from the region a, because it is due to an excess energy in the wind that may destroy the turbine structure.

In the region of rated power (c) and the region (d) of no power, limiting the turbine speed is challenging. This can be achieved by two different way of aerodynamic control. First is stall control. The wind turbine of this type has its blades fastened to the hub at a fixed angle. It uses the aerodynamic principles in the design of the blades. So, if the wind speed increases,

turbulence occurs on the back of the blade which helps to suppress the acting lifting force on the blades.

The second way is the pitch control. Wind turbines of this type have their blades connected to the hub by actuators where the pitch angle can be changed in response to the wind speed. By sensing the produced power, the controller send a signal to the blade actuators to change the pitch by a fraction of a degrees to make the blades facing the wind direction.

Although there is always an ambition for increasing the rated speed of wind turbine, this cannot always be achievable because of the restrictions in manufacturing the noise level which occurs by the rotating blades of the turbine. Consequently, the blades tip speed is limited to 70 m/s for onshore turbines whereas with offshore turbines the noise level is not an important issue (Polinder et al. 2005).

## 1.2.Problem Statement

The control of the wind turbine is the major subject of this research. A small off-grid horizontal axis wind turbine for residential uses presented by (González et al. 2011) shall provide the theme problem. It can be seen as a multivariable process of two controlled outputs (turbine angular speed and electrical generated power), with two manipulated inputs (the generator field current and the blades pitch angle) and random disturbances.

Multivariable systems have some limitations which do not exist in the classical systems of single input single output particularly the interaction issue between the inputs and outputs. Otherwise, a single input affects multiple outputs or multiple input affect a single output.

The interaction can be seen as a degrading to the system performance since most of systems has this inherent nature.

In addition to system interaction, random disturbances are expected which is considered during the controller design stage. This could be from the variations in wind speed or changes in the connected load.

Wind turbines control design has many necessities to be reflected but the less interacted cheap control is always an important target, since the controller can help in generating more power and limiting the rotor speed to optimum values extending the life of the turbine structure.

### 1.3. Research Objectives:

This research aims to design two multivariable controllers, the first one was first introduced by Whalley and Ebrahimi (2004) which stressed designing a controller with least effort dissipated (Least Effort Controller) and the second one is based on the H-infinity theory which was initially presented by Zames (1981). Both controller achieve the following:

- Maintaining the system stability in the closed loop mode.
- Improving the transient and steady state responses.
- Inputs-outputs interactions to be less than 10%.
- Disturbance rejection to be enhanced.
- Controller Energy consumptions to be enhanced.

After that, a comparison study is provided showing the following:

- Disturbance suppression achieved by each controller.
- Complexity of each controller.
- Energy dissipated by each controller.

## 1.4. Research Organization

The proposed research is about designing a multivariable controllers and comparing between them. In chapter one, the reader has an overview of the plant for a Horizontal Axis Wind Turbine, the problem statement, research objectives and the research organization.

Chapter two is a literature review and it is divided into four sections, the first one is the background of automatic control history and the three others are about wind turbine dynamics and control methods. Then the least effort controller and H-infinity methodology, respectively will be studied.

The materials of chapter three present mathematical modelling of the plant where the transfer function is obtained, and the design procedure for the both controllers is examined. In brief, this chapter is a theoretical basis for the next chapter.

Chapter four shows the implementation of both controllers on the obtained transfer function of the plant. It deals with the simulation results and performance of each controller individually. Then, a comprehensive comparison study is presented between the two controllers.

In conclusion, chapter five ends the research with a conclusion on the two controllers showing advantages. Recommendations for future work are suggested.

## Chapter II

### 2. Literature Review

#### 2.1. Automatic Control

Automatic feedback theory is a versatile, general field of study known for more than 2000 years (Stuart Bennett). Because of that, it can be used in technology, economics, sociology and biology.

In 1967, The British Standard Institution defines the term closed-loop control system as "a control system possessing monitoring feedback, the deviation signal formed as a result of this feedback being used to control the action of a final control element in such a way as to tend to reduce the deviation to zero." Moreover, It specifies feedback as "the transmission of a signal from a later to an earlier stage."

The Feedback theory has deep roots in the history prior to the 19<sup>th</sup> century. Although, James Watt invention of the Centrifugal Governor which in 1788 and was widely accepted all over the world. However, feedback theory extends beyond that period.

Back to the first half of the third century B.C, in the city of Alexandria, a mechanician named Ktesibios was the inventor of the water clock. He used a valve to regulate the flow of water in

spite of water level changes. For that, Ktesibios may be considered the inventor of the first feedback device.

One generation after Ktesibios, Philon used another method for regulating liquid level which composed an elementary on-off control (Myr 1970).

In the first century of A.D., Heron whose main works were in mechanical engineering, described the feedback devices in his book “Pneumatica” which adopted the Ktesibios float valve. He controlled a wine dispenser by rising and sinking of a float.

Subsequently, there had been several books describing water clocks with float valves. The most famous ones and available to the present days are: Pseudo-Archimedes, the works of Al Jazari and the book by Ibn Al Saati, (Myr 1970).

In the 9<sup>th</sup> century in Baghdad, Banu Musa collected descriptions of one hundred pneumatic and hydraulic devices in a book called “Kitab al-Hiyal”. In that book, descriptions of oil lamp level float valves models can be found.

Long after that in Europe after 1600, the first feedback system was invented. This was the temperature regulator of Cornelis Drebbel in Holland. In 1681,

Denis Papin used a pressure cooker where the pressure is regulated by a weight-loaded valve. After that in 1707, the same device was used by Papin but as a safety valve on a high-pressure steam engine. A more complicated pressure regulator was used by Robert Delap in 1799. Three months later, Mathew Murray enhanced the Delap regulator to avoid some shortcomings.

Besides Delap and Murray pressure regulators, Boulton and Watt used another kind of pressure regulator which was employed for steam engines in Paris in 1830.

In addition to the level, pressure regulators and thermostats various types of regulators were constructed by millwrights. One of them is the Mill-Hopper, which is considered by some science historians as the oldest feedback device. In this invention, the quantities of grain provided to the millstones is directly related to the speed of the mill. In contrast, there are arguments and objections that changing in grain supply is in the system and is not achieved deliberately and was not designed for it so it should not be considered as a feedback device. Millwrights have many contributions and inventions in the feedback devices in the 18<sup>th</sup> century. Unfortunately, most of these contributions have no record except the one registered as patents. One of those patents is the British patent of the blacksmith Edmund Lee in 1745, he invented the Fan-tail. The Fan-tail is an accessory to the wind mill designed to help the mill to keep facing the wind, (Myr 1970), Figure 2-1.

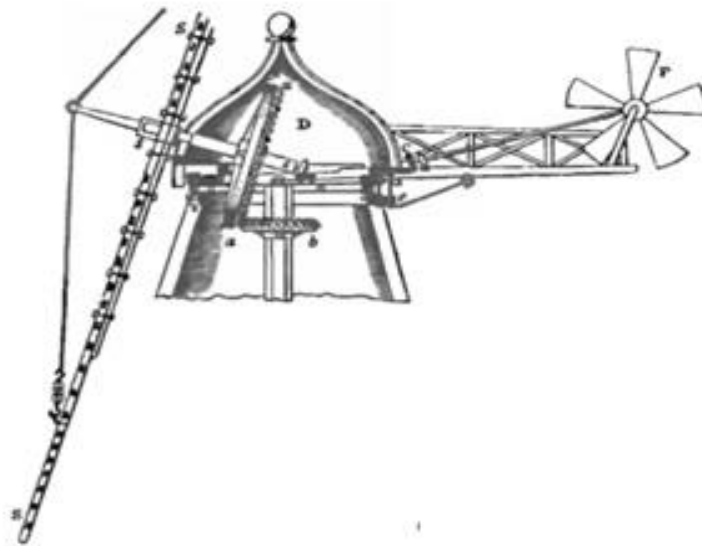


**Figure 2-1, Fan Tail (Myr 1970).**

The devices used for regulating the speed of windmills, is the self-regulating windmill sail. Edmund Lee was the inventor of that device. The aim of the self-regulating windmill sails is to keep the mill speed constant regardless of the changes in the wind speed. Although succeeding in achieving constant speed, still the device is not fulfilling the feedback criteria because maintaining the speed of the mill was not achieved by the sensing of the wind speed but it was by the effect of the change in the torque due to the change in wind speed. For that, a number of mechanisms and techniques were used to detect the wind speed and produce a force for keeping the mill stones gap. The most famous and significant ones were invented by Thomas Meads. Those devices were based on the principle of the centrifugal pendulum which was used to sense the wind speed Figure 2-2, this regulator opened the way for the centrifugal governor.

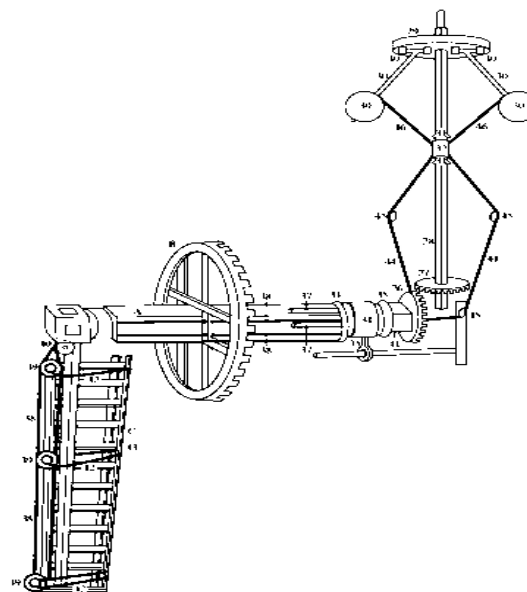


**Figure 2-2, Mead's speed regulator**

During the 18<sup>th</sup> century, the most important contributions in control was the steam engine governor by James watt who utilised Mathew Boulton's lift-tenter which was used to control the spacing between grinding stones in wind and water mills.

**"The centrifugal governor** is based upon the rotating pendulum adopted from the millwrights, where flyweights perform a centrifugal motion depending on the speed of revolution. By appropriate mechanical elements this motion is transmitted to the inlet valve of the steam engine so that by throttling the steam flow the speed is reduced." (Myr 1970).

Later and in 19<sup>th</sup> century, with the spreading of the centrifugal governor some problems floated on the surface. For example, the governor could not remove the offset because it has no integral action. Another problem was the response for load changes. A number of efforts to overcome those problems were attempted. At the end of the century, many governors were effective and available but for steady state designs. In contrast, few scientists were interested in the analysis of the feedback system dynamics.

In the same era, some British scientists became concerned with the governor stability in order to maintain the direction of the telescopes which resulted in a formal study by George Bidell Airy in 1840, (Nof 2009).

After that, in 1868, James Clerk Maxwell studied the governor dynamics for keeping the rotational speed of a coil constant. He derived a third order linear system and the precise conditions of stability from the coefficients of the characteristics equation. On the same time, Maxwell left for mathematicians the stability analysis of systems of higher order. In 1877 Edward James Routh won the Cambridge University Adam Prize for mathematics. Routh was concerned with stability analysis for many years and he succeeded in obtaining a solution for fifth order systems.

In 1895, Adolf Hurwitz used the coefficients of the polynomial and arranged it in a square matrix which has been called Hurwitz matrix. Using the Hurwitz Matrix and the determinants of its submatrices, Hurwitz showed that "the polynomial is stable if and only if the sequence of determinants of its principal submatrices are all positive" (Hurwitz 1895).

At the beginning of the 20<sup>th</sup> century, textbooks started to appear of the subject of the stability and regulation mainly on the prime movers regulation. One of the most important books was for Tolle's "Regelung der Kraftmaschine" book which influenced the subject of control theory for almost two decades (Bennett 1986).

In 1922, Nicholas Minorsky designed the control law for position control systems and presented the PID controller.

In 1936, the first group to study the automatic control was Industrial Instruments and Regulators Committee which was formed by the American Society of Mechanical Engineers. After that, in 1940 field-adjustable instruments with PID controllers were under operating. After that, in 1942, Zeigler and Nicholas of the Taylor Instrument Companies presented various papers for providing a procedure for optimum settings of PID controller which is called Ziegler-Nicholas tuning rules.

In 1951 in England and after that 1953 in New York, two conferences were held for the subject of Automatic Control starting a new era and which was the beginning of the modern control theory studies. In Germany 1956, another conference on the subject of Automatic Control was held. Those conferences played a big role in guiding the direction and transition of the Automatic Control theory. Besides that, in 1960, the Moscow conference was a significant one in showing how deep the multivariable feedback problem is. Particularly because of the presented paper of Kalman "On the General Theory of Control Systems". Moreover, the Kalman

paper emphasizes on the difference between the multivariable feedback control and multivariable feedback filter. His work approached the plant in the state space domain and presented the optimal control problem, which used the quadratic performance index.

Although Kalman optimal control method was powerful, it could not be applied generally on the various industrial systems since the plant cannot be modelled accurately. Moreover, the complexity in designing the performance index formula and Kalman filter for those systems returned the interest in the frequency response approach which was used for multivariable systems in 1966 by Howard Rosenbrock, (Bennett 1986).

## **2.2.Wind Turbine**

Since early history, human beings have benefited from the energy of wind. Five thousand years B.C, It has been utilized in propelling boats in Egypt and after that in pumping water in Persia. But using it to generate electricity was started in the 19th century when Charles Brush used a DC wind power turbine to generate 12KW of electrical power in Cleveland as did professor James Blyth in Scotland in 1887. In 1890, wind power helped north America to generate power for homes and businesses for farmers and later in the same era, between 1846 and 1908, meteorologist, Poul La Cour who was concerned with electricity storage built his own wind turbine to produce electricity to help producing hydrogen which he used for the lighting of his school ("The Wind Energy Pioneer - Poul la Cour" n.d.). After that, Denmark used first 23 m diameter wind turbine to generate electricity using the principle of aerodynamics. By 1910, hundreds of wind turbines were generating electricity across Denmark. After that, in 1925, Marcelleus and Joseph Jacobs started the first high speed battery charging wind turbine. Between 1940 and 1950 during the World War II the F.L. Smidth Turbines Company in Denmark played a significant role in generating Direct Current (DC). In 1951, the DC generator was replaced

with the AC asynchronous generator. The interest in using wind turbines to generate electricity has increased in 1970s because of the oil crisis (Hemami, 2012). In the early eighties, thousands of wind turbines were manufactured in Denmark and California using the Danish origin which was a breakthrough in the wind turbine industry. From that era until 1992, wind turbine commercial use did not exceed 225 kilowatts but due to advancements in technological sectors, wind turbine blade materials and electrical conversions systems the generated power increased. Moreover, in 2005 the generated power from wind turbine achieved a significant record (6183 megawatt) and Denmark generated 20% of its electricity need from wind power.

In most of wind turbine design, the wind mass is considered uniformly distributed around the blades. Because of that, the control process for one blade is applicable for the others. On the other hand and due to the uncertainty of the wind speed the wind turbine rotor is running at variable speed with no limitations or optimization if no control is applied. Early, wind turbines were designed to run on constant speed regardless of the wind speed. This gives the system simplicity in design, control and operation but with low efficiency and low power. Moreover, fixed speed wind turbines don't react to the wind changes which leads to damaging in the turbine structure at higher wind speeds.

Variable speed wind turbines are now connected to the AC electrical power grid. Recently and because of the advancements in the power electronics, a power regulation becomes an affordable task. Several methods have been used to transform variable voltages and frequency to a constant regulated voltage and frequency. Some of the early attempt to used methods for connecting a diode rectifier to rectify the variable frequency output of a permanent magnet generator.

Using the power electronics in the variable speed wind turbine increases the overall cost. However, the cost of the variable speed technology has a promising future and is the best in capturing more energy and reducing the fatigue on the turbine structure.

### 2.2.1. Wind Turbine Control

As presented in the previous section and with the distinction of the rotor types, which may be of variable speed or limited to a constant speed, the wind turbine is classified as a Fixed Speed Wind Turbine FSWT or Variable Speed Wind Turbine VSWT.

Early in 1970, FSWT was being used due its simplicity and cheap generators of fixed speed depending on the frequency of the existing at electrical grid (martinez 2007). However, fixing the speed of the turbine at the frequency of the electrical grid, the turbine efficiency is very low since it is not optimizing the use of the wind.

Allowing the turbine to rotate at variable speed, makes the rotor aerodynamics optimum where its speed is proportional to the wind speed. The aerodynamic efficiency of the wind turbines depends on the rotor design and shape airfoil, blades length, speed in rpm and angle of attack (National Renewable Energy Laboratory 2001).

Because of that, the wind turbine can be controlled by changing the speed or the pitch angle of the blades. So, the four different configurations of wind turbine are:

- **Fixed-speed and fixed-pitch:** this configuration was the foremost used for long time where the electrical generated is connected directly to the existing power grid. It is called fixed speed because the speed of the generator is limited by the frequency of the grid. Also, it is called fixed pitch because the pitch of the blades is not controlled and controlling the blades is done inherently in the design process of the blades where the stall effect is preventing the turbine blades to rotate with speed above the design speed. Figure 2-3 depicts the stall effect.

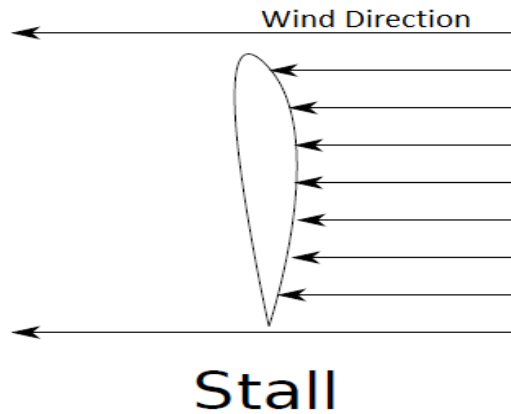


**Figure 2-3, Stall Effect**

This configuration of wind turbine makes it very poor in power generation efficiency and performance.

- **Fixed-Speed-Variable-Pitch:** clearly from the names, the fixed speed affects the power generation when the wind speed is below the rate. On the other hand, when the wind speed exceeds the limit, the power is controlled by pitching the angle of the blades which gives more efficiency in the higher wind speeds. This type was used in the medium size wind turbines.
- **Variable-Speed-Fixed-Pitch:** this setup is suitable for areas of low wind speed profile. Consequently, the pitch angle of the blades is optimum. Operating with variable speed makes the power generation of higher efficiency but with a drawback of adding component to the wind turbine to match its variable frequency with the grid frequency. Consequently, this configuration increases the cost of the turbine. Although of that and because of its high power conversion efficiency, this type of turbine is widely commercially used in the areas of low wind speed profile.

- **Variable-Speed-Variable-Pitch:** this setup is the most common one in the commercial sector. Where it can work in all the wind speed regions. Figure 2-4 shows the wind speed regions.

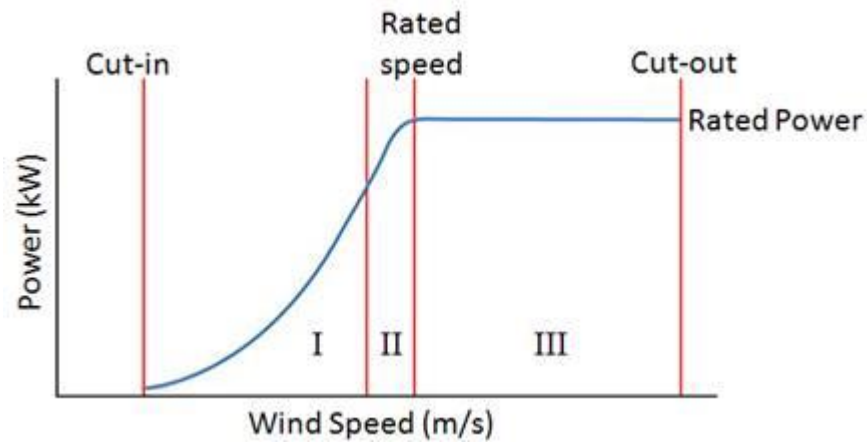


**Figure 2-4,** Wind Speed Regions

Because of the uncertainty of the wind speed, Wind Turbines have to respond to the wind speed as required whether the response is limited or optimized. So, the operating regions of the wind turbine are classified in three main regions. Below the rated speed, above rated speed and in the middle of both. In addition to that, two other regions the wind turbine has to stop operation due to the non-feasibility of the turbine operation where the wind is very low and has insufficient energy to produce power or the wind is very fast which could damage the turbine structure (cut out region). All of that is achieved by the Variable Speed, Variable Pitch Wind Turbine.

Wind Turbine efficiency does not only depend on optimising the use of wind speed to generate power, but the electrical conversion system is an important component in the wind turbine. The electrical conversion system is the type of generator along with power electronics used to convert the rotational speed to electricity.

For a Fixed Speed Wind Turbine, the squirrel-cage induction generators SCIG are the common used. Then SCIG is connected to soft-starter which is in turn connected to a capacitor

bank. The previous topology is called the "Danish Concept" (Munteanu et al. 2008). Figure 2-5 depicts the described Danish Concept.

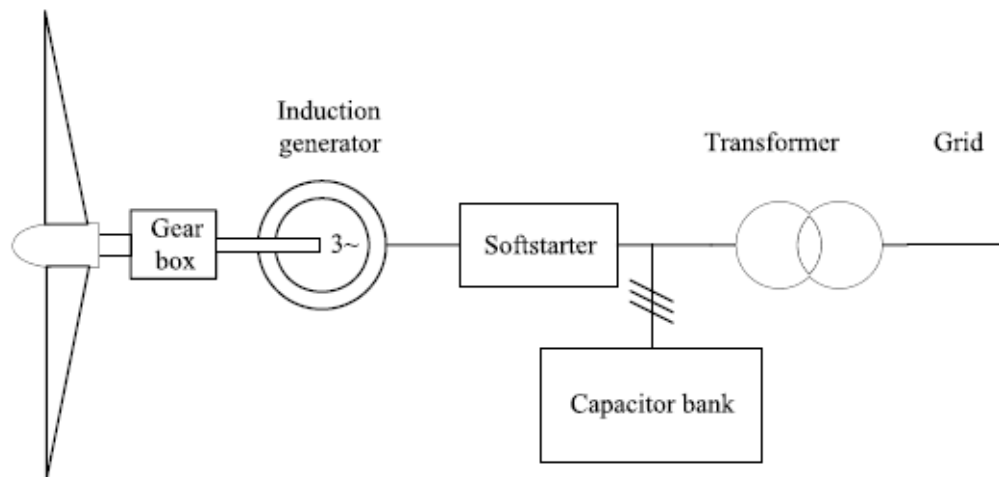


**Figure 2-5,** General Structure of a FSWT of Danish Concept (Munteanu et al. 2008)

At any wind speed, this Danish Concept WT has to operate at constant speed. This speed is synchronised with the electrical grid frequency. Which means that, the WT system is more dependent on the mechanical subsystem for wind gusting. A peak in the electrical output can be observed. This concept needs a strong structural design which means expense especially at high-rated power and furthermore it has limited controllability since the rotor speed is fixed (Muller, Deicke & De Doncker 2002).

However, the SCIG has many advantages such as high efficiency, simple construction and low maintenance costs. The capacitor bank shown in the above figure, is necessary to maintain high power factor while the softstarter is to smooth the current surge in case the wind turbine system is connected to the electrical grid (Munteanu et al. 2008).

Apart from that, modern high-rated power wind turbines work at variable speeds, which needs a more complicated electrical system to effectively respond to fluctuations in wind speed.

The most common types of electrical system for variable speed wind turbines VSWT are:

- Direct in line generator system: or sometimes called full variable speed conversion system. As depicted in Figure 2-6, a synchronous generator is used as a conversion system connected to a DC bus which is power converter to maintain the required frequency for grid interfacing. From this scheme, the power can be generated reaches 1.5 MW. In contrast there are various downsides for this implementation. First, the expensive power converter used in this scheme. Second, the using of converter filters are also expensive. Finally, the converter efficiency which affects the total wind turbine system efficiency.

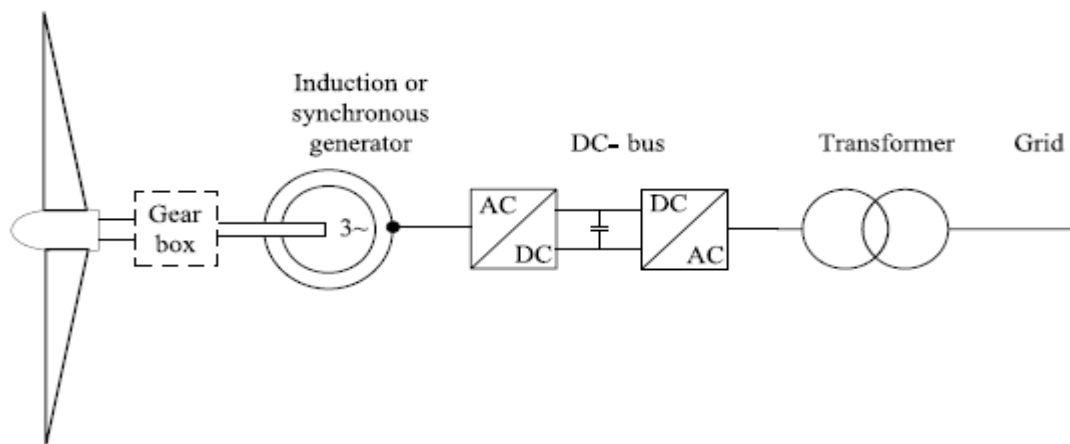


**Figure 2-6, Direct in Line Wind Turbine System**

- Doubly Fed Induction Generator: its scheme implementation is shown in Figure 2-7. Which is used and developed to overcome the previous mentioned type. Therefore, it has several advantages which can be summarized as: lower cost and more efficiency (Muller, Deicke & De Doncker 2002).

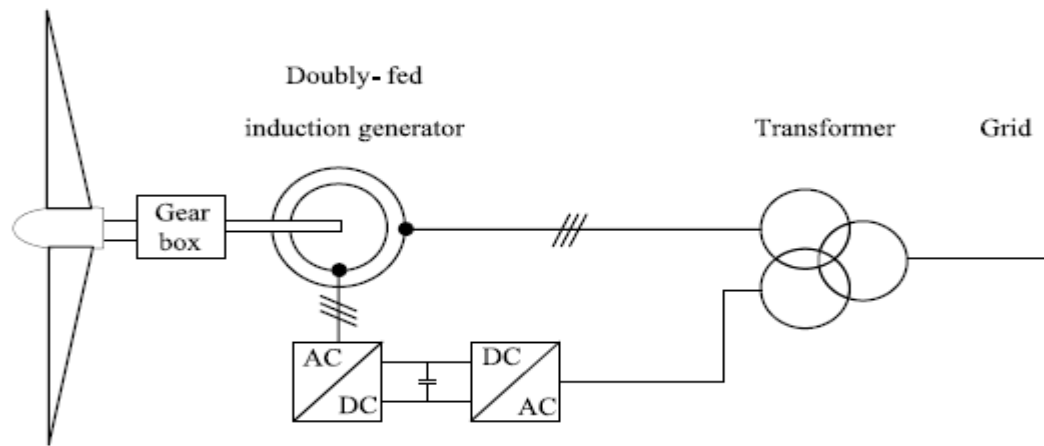


**Figure 2-7,** Doubly Fed Induction Generator Wind Turbine System

### 2.2.2. Wind Turbine Dynamics

The basic principle of the wind turbine can be presented by an aperture perpendicular to the wind direction. The aperture opening is of a cross sectional area  $A$  as shown in **Figure 2-8**.

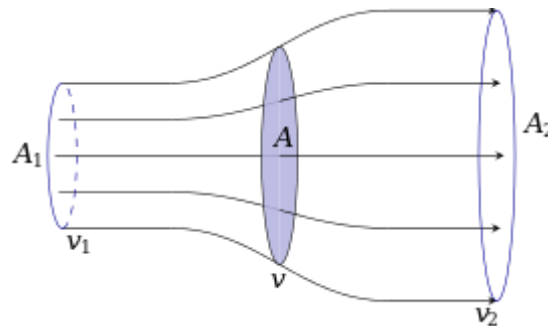


**Figure 2-8**, Wind passing through an aperture

The rate of change of the wind mass passing through the aperture can be calculated by the following equation:

$$\dot{m} = A * v * \rho \text{ kg/s}$$

where  $v$  is the wind speed and  $\rho$  is the wind density.

As known, any moving mass has a kinetic energy which is proportional to its velocity squared as the following  $v^2/2$ . In the above aperture, the wind kinetic power passing through the aperture can be calculated as the following:

$$P = \frac{1}{2} v^2 * A * v * \rho = \frac{1}{2} \rho A v^3 \text{ watt}$$

This power passing through an opening, space, or aperture can be collected by blades which convert the wind power.

From the above equation, it can be shown that, the wind power basically depends on three significant factors which are: the air density, the swept area, and the wind speed.

Air density can be calculated by considering the air as an ideal gas, and the ideal gas density depends on the ambient temperature and pressure.

The following equation shows the ideal gas density:

$$\rho_{dry\ air} = \frac{p}{R \cdot T}$$

where  $p$  is the atmospheric pressure in Pa.

$T$  is the atmospheric temperature in Kelvin.

And  $R$  is the specific gas constant of the dry air which is  $287.05 \frac{J}{(kg.K)}$

At sea level, the atmospheric pressure as per the international standards is 101.325 kPa, for temperature of  $20^\circ$  the calculated pressure as per the ideal gas equation is  $1.204 \frac{kg}{m^3}$

Referring to the wind power equation, and considering the previously mentioned atmospheric conditions. It is assumed that the wind speed would be 10 m/s then the possible power could be 600 watt for every square meter of swept area.

On the other hand, the power from wind is limited which means it is impossible to utilize the full power available. This is because, the wind speed passing through the blades doesn't converge to zero. So in the ideal conditions, the maximum utilized wind power cannot exceed the limit of  $16/27$  (59.26 %) which is called the Betz Coefficient, named after the German engineer Albert Betz (Blackwood 2016). In other words, the power coefficient of any turbine is the ratio between the power produced by the wind turbine and the full wind power which will never exceed the Betz limit.

The blades of wind turbines (propellers) have an airfoil of a cross section as shown in **Figure 2-9, Aerofoil cross section**

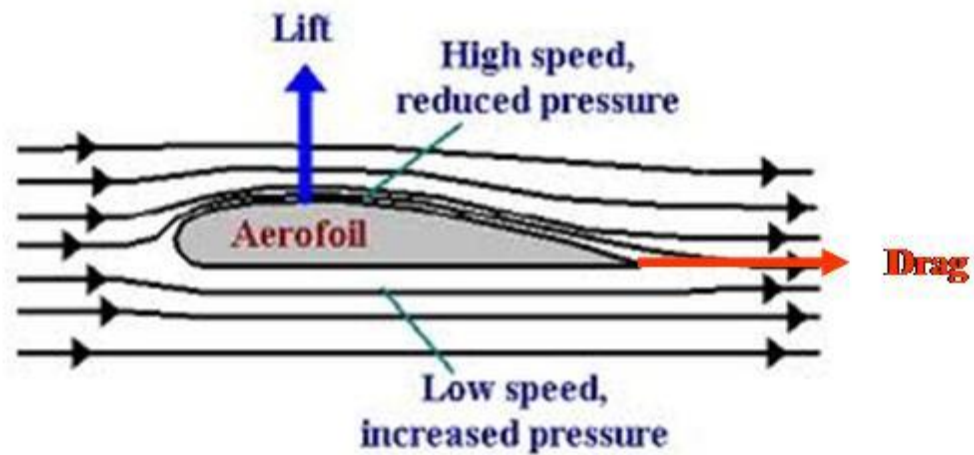


**Figure 2-9**, Aerofoil cross section

As depicted in the above figure, at the top of the aerofoil the wind speed is higher than the bottom of the aerofoil. This speeding up is natural in order to compensate for the obstacle in the face of the passing air. As per Bernoulli's principle which states that "an increase in the speed of a fluid occurs simultaneously with a decrease in pressure or a decrease in the fluid's potential energy" the result in increasing the wind speed leads to decreasing of the wind pressure at the top of the airfoil which produces lift force (vertical on the wind direction) . In contrast, the speed on the bottom of the airfoil decreases and allowing slight increase in the wind pressure which can be neglected. Furthermore, the drag force (parallel to the wind direction) appearing is due to the turbulences on the airfoil.

Since the blades are moving parts of the turbine, the wind direction will not stay along the cord line, Figure 2-10. This reflects a decrease in the air pressure which counters act the lift force on the blades. This effect can be avoided by keeping the blades at an angle from the wind stream which is called the pitch angle.

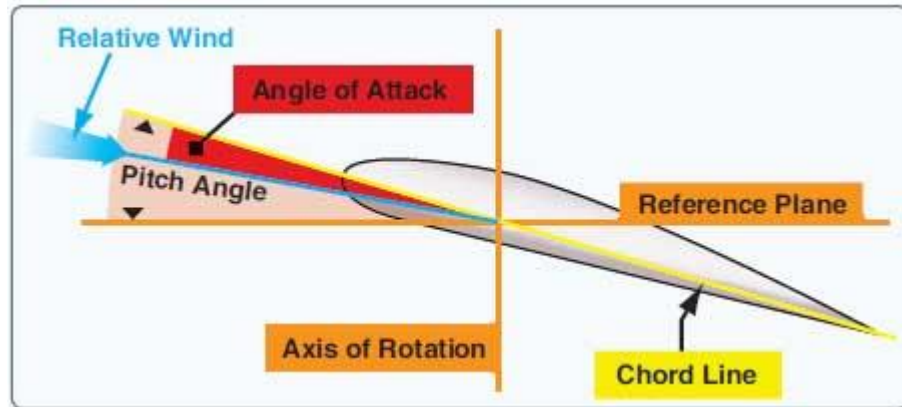


**Figure 2-10**, Pitch angle and relative wind

The best pitch angle for higher rotating speed can be achieved by keeping the relative wind direction in tangency with the lower side of the airfoil.

The transitional movement of the airfoil changes as its distance from the rotation centre (Akbarzadeh 1992) which can be calculated from the following equation:

$$v = r\omega \text{ in } m/s$$

where  $r$  is the radial distance in meters and  $\omega$  is the angular velocity of the blades.

Due to the variety of the transitional motion of the blades, the relative wind speed and the chord line are in parallel only in one radius. So, for different radii, the chord line and relative wind speed direction will be an angle which is called the “Angle of Attack”, Figure 2-10.

This angle of attack has a significant effect and cause in creating turbulences on the blades. And this is why the twisting in the blades is necessary.

The twist in the blades leads to non-constant pitch angle. Therefore, the manufacturer designers take that into consideration by calculating the optimum required pitch angle which is can be done by using the following equation:

$$\tan \beta = r\omega/v_w$$

where  $\beta$  the pitch angle, and  $v_w$  is the wind speed.

The wind turbine blades are designed based on the rated wind speed of the wind turbine. Moreover the wind blades efficiency will not meet the design if the wind speed exceeds the rated wind speed which means a change in the value of  $\omega/v_w$ .

For avoiding that risk, modern wind turbines are equipped with actuators to rotate the blades around their axis to change the pitch angle which results in an optimum wind turbine.

### **2.3. Least Effort Regulation.**

Least Effort regulation technique is proposed by Whalley and Ebrahimi in 2004, where the regulation of the input reference point and disturbances is considered. Their strategy was achieved by using feedback an inner and outer loop.

In (Whalley & Ebrahimi 2006), a controller method for multivariable systems is explained, by employing output feedback, passive compensation and proportional regulation. Furthermore, using of integrators in their design procedure is avoided.

Their design process has two aims:

- Securing the closed loop dynamic response by means of inner-feedback loop.
- Low steady state output coupling by pre-compensation and outer-loop gain settings.

This desired performance is attained while using the minimum control energy which means, minimum wear, maintenance costs, least heat, least costs and least vibration.

Whalley and Ebrahimi provided application study proving their strategy and comparing it with other controllers which included Inverse Nyquist Array, Characteristic Loci and Perron-Frobenius methods.

## 2.4.H-infinity Method.

In classical methods, the main techniques were focused on altering the system parameters and using graphs to check the system response.

By the time, the control theory aim became not only to stabilize the system or adjusting the output response based on reference inputs, the need of optimizing worst-case error an important issue. This started in the circuit theory where an amplifier is designed with a maximum gain with a prescribed frequency bandwidth. This was done by the H infinity theory, which is focusing on the worst response in the frequency domain.

The first scientist who introduced the H infinity theory in the MIMO systems was G.Zames by formulating a feedback problem as an optimization problem with an operator norm which is highlighted in (Zames 1981).

Zames based his design approach on using weighted seminorm on the algebra of operators to examine the sensitivity of the plant and he used the principle of approximate inverse to reduce the sensitivity of the plant. Lead-lag networks of classical control theory had been used to optimize the sensitivity. Moreover, Zames obtained general answers for the effect of the plant invertibility on the feedback, measures of the plant uncertainty for optimization and the using of plant uncertainty to design a feedback.

In 1984, John C. Doyle introduced the first solution of multivariable H-infinity problem relying on state space method.

Between 1988 and 1990, P. P. Khargonekar, I. R. Petersen, M. A. Rotea, and K. Zhou presented that, for the state feedback H-infinity problem a sub-optimal controller can be chosen

as a constant gain and the state feedback matrix is introduced as an Algebraic Riccati Equation solution.

In 1989, John C. Doyle, K. Glover, Khargonekar, B. A. Francis established a procedure for solving an H-infinity problem using state space. In the same era, K. Glover and D. C. McFarlane presented the H-infinity loop shaping method which is considered a systematic method for finding sensitivity functions that guarantee the system performance and robustness against model uncertainty and disturbances.



- Gearbox: transforming the low speed shaft to the high speed shaft.
- Electrical generator: AC geared synchronous type.
- Connected load.
- Pitch controller to control the angle of attack of the wind by rotating the blades.

Some assumptions are made such as: the turbine tower is rigid, the shaft stiffness and damping are ignored to simplify the model and avoid non linearity in the system. In addition, high speed shaft torque is equal to the generator torque.

### **Mechanical model of the WT:**

In order to describe the mechanical model of the system, the forces and torques causing the movement need to be shown. Figure 3-1 shows how the movement is transferred as the wind hits the blades, moves the low speed shaft which transformed to a high speed by passing through the gearbox to generator shaft which causes the electric conversion system (synchronous generator in this study) generates electricity.

Three main equations can be used to describe the mechanical components of the wind turbine taking in consideration some assumptions explained earlier.

From the low speed shaft which is connected to the blades:

$$J_r \dot{\omega}_r = \tau_a - B_r \omega_r - \frac{\tau_{hs}}{N} \quad 3-1$$

where  $J_r$  is the rotor inertia,  $\omega_r$  is the angular speed of the rotor,  $B_r$  is the viscous friction coefficient,  $\tau_a$  aerodynamic torque from the wind,  $N$  the gearbox ratio and  $\tau_{hs}$  the torque of the high speed shaft.

Gearbox ration is  $N = \frac{\omega_g}{\omega_r}$

In the high speed shaft the system results in the following equation:

$$J_g \dot{\omega}_g = \tau_{hs} - B_g \omega_g - \tau_{em} \quad 3-2$$

where  $J_g$  is the generator inertia,  $B_g$  is the friction coefficient and  $\tau_{em}$  is the generator magnetic field torque which is opposite to the generator torque.

Using the above low speed and high speed shaft equations and considering the rotor angular speed  $\omega_r$  the wind turbine dynamics could be represent in one equation. In order to obtain that, gear ratio effect needs to be considered showing how the damping, torque and inertia are converted between two shafts.

Since,

$$J_r = \frac{J_g}{N^2} \text{ and } B_r = \frac{B_g}{N^2}$$

adding equation (3-1) and (3-2) gives:

$$J_r \dot{\omega}_r + J_g \dot{\omega}_g = \tau_a - B_r \omega_r - N \tau_{hs} + \tau_{hs} - B_g \omega_g - \tau_{em}$$

$$J_r \dot{\omega}_r + N^2 J_g \dot{\omega}_r = \tau_a - B_r \omega_r - N \tau_{hs} + \tau_{hs} - N^2 B_g \omega_r - \tau_{em}$$

$$J_t \dot{\omega}_r = \tau_a - B_t \omega_r - \tau_g \quad 3-3$$

Where,  $J_t = J_r + N^2 J_g$ ,  $B_t = B_r + N^2 B_g$ , and  $\tau_{hs} = \tau_g - N \tau_{em}$

### Electrical model of the wind turbine:

The electrical conversion system in this research is a synchronous electric generator which contains a rotor (the high speed shaft of the turbine) and a stator (the stationary part). The Generated power  $P_g$  is proportional to the voltage across the stator terminal  $E_g$ . This results in a voltage proportional to the generator angular speed  $\omega_g$  and also the generator field current  $I_f$ , as per the following equation:

$$E_g = K I_f \omega_g$$

The excitation magnetic field is achieved using an electro-magnets fed by external DC source which enables controlling the field current  $I_f$  of the generator rotor.

By assuming the connected load is pure resistance  $R_L$  and the generator reactance is  $X_g = \alpha N \omega_r$ , the generator power as follows:

$$P_g = \frac{E_g^2}{R_L} = \frac{K^2 R_L I_f^2 \omega_g^2}{(R_L^2 + (\alpha N \omega_r)^2)}$$

From the above power, generator torque can be calculated as follows:

$$\tau_g = \frac{P_g}{\eta_g \eta_m \omega_g}$$

where  $\eta_g$  and  $\eta_m$  are electrical and mechanical efficiencies of the generator, respectively.

In the other hand, the aerodynamic torque  $\tau_a$  depends on the wind turbine characteristics, which can appear in the torque coefficient of each turbine.

By theoretical and experimental analysis, the wind turbine aerodynamic torque can be represented as following:

$$\tau_a = 0.5 \rho \pi R^3 v^2 C_q(\lambda, \beta)$$

where  $R$ =rotor radius,  $v$ =wind velocity and  $C_q(\lambda, \beta)$  is the torque coefficient which depends on tip speed ratio  $\lambda$  and pitch angle  $\beta$ .

In summary, the complete system can be represented in four core equations which are:

$$J_t \dot{\omega}_r = \tau_a - B_t \omega_r - \tau_g \quad 3-4$$

$$\tau_a = 0.5 \rho \pi R^3 v^2 C_q(\lambda, \beta) \quad 3-5$$

$$P_g = \frac{E_g^2}{R_L} = \frac{K^2 R_L I_f^2 (N \omega_r)^2}{(R_L^2 + (\alpha N \omega_r)^2)} \quad 3-6$$

And

$$\tau_g = \frac{P_g}{\eta_g \eta_m \omega_g} \quad 3-7$$

The above model is linearized based on first order Taylor series. Which led to the following Laplace representation of the system:

$$\begin{bmatrix} W_r \\ P_g \end{bmatrix} = \begin{bmatrix} g_{11} & g_{12} \\ g_{21} & g_{22} \end{bmatrix} \begin{bmatrix} I_f \\ \beta_{ref} \end{bmatrix} + \begin{bmatrix} g_{13} \\ g_{23} \end{bmatrix} V + \begin{bmatrix} g_{14} \\ g_{24} \end{bmatrix} R_L \quad 3-8$$

In this thesis, the transfer function from the wind speed  $V$  and resistive load  $R_L$  is ignored and the both inputs are considered as disturbances.

After applying system parameters and finding the operation point for inputs and outputs, the system transfer function of the system becomes:

$$\mathbf{G}(s) = \begin{bmatrix} \frac{-70.55}{15s+0.233} & \frac{-1.56}{30s^3+15.47s^2+2.48s+0.035} \\ \frac{3458s+173.1}{15s+0.233} & \frac{-8.05}{30s^3+15.47s^2+2.48s+0.035} \end{bmatrix} \quad 3-9$$

## 3.2. Open Loop Response

By using the transfer function shown in equation 3-9, the open loop block diagram is created using SIMULINK, Figure 3-2.

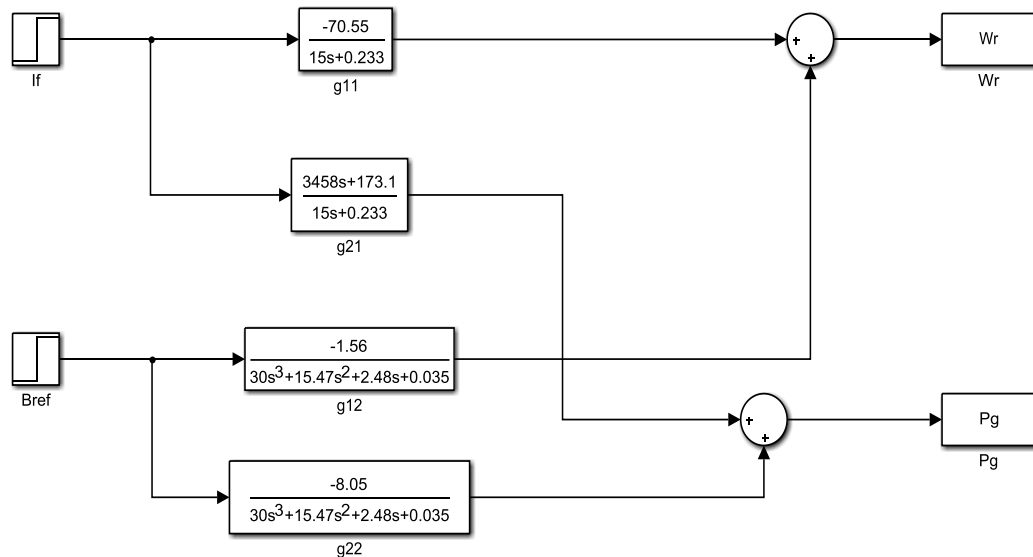


**Figure 3-2,** Open Loop Block Diagram

First, a step change is applied on the first input ( $I_f$ , field current) and the output is depicted in Figure 3-3. The figure shows a slow response where the system needs more than 350 seconds to reach its steady state value.

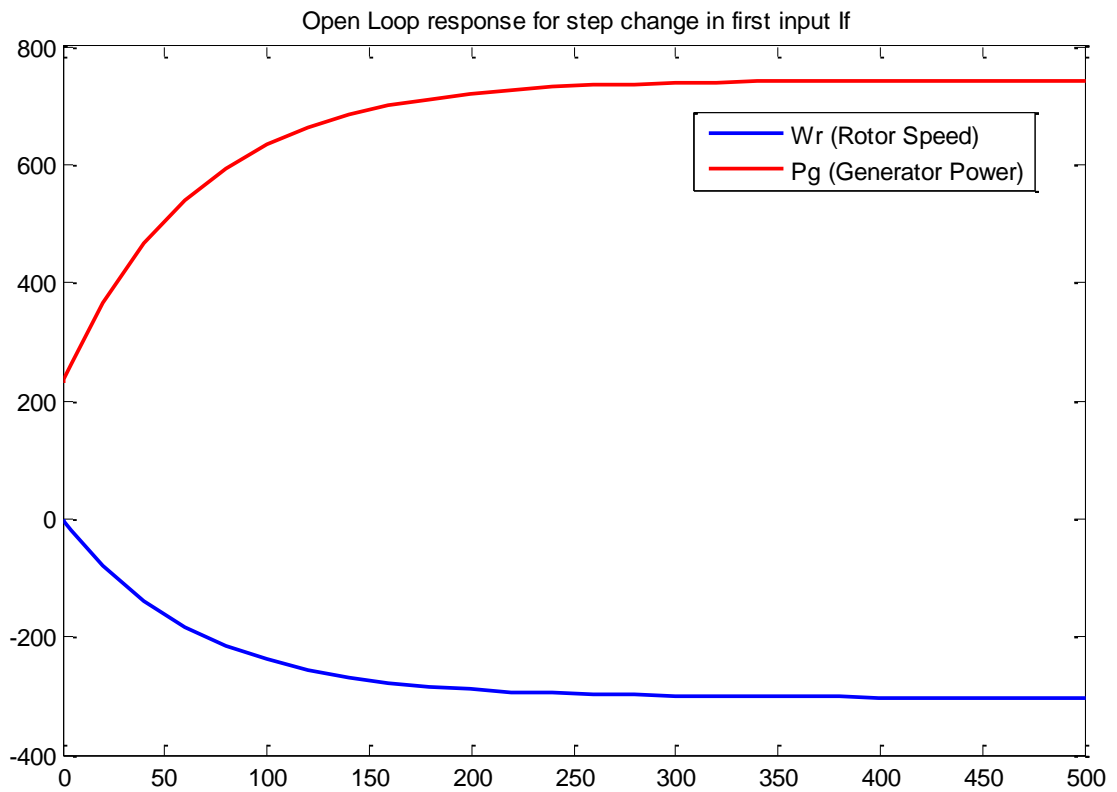


**Figure 3-3**, Open Loop Response for a step change in the first input

On the other hand, a step change is applied on the second input ( $B_{ref}$ , pitch angle), Figure 3-4 displays a slow response reaching steady state after 350 seconds too.

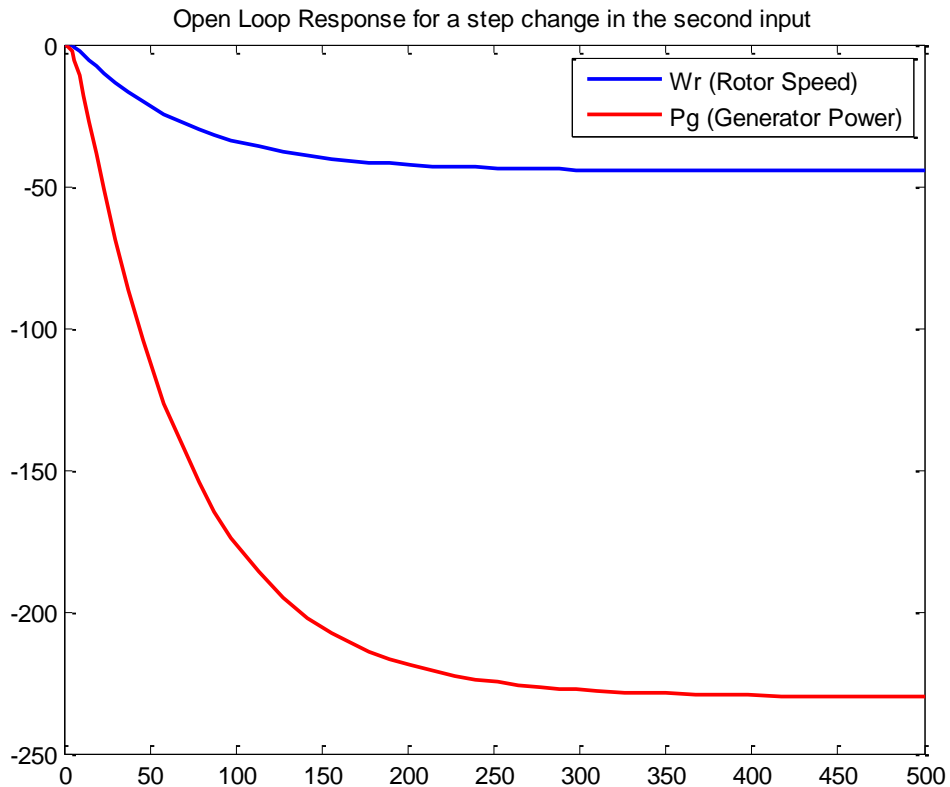


**Figure 3-4,** Open Loop Response for a step change in the second input

Furthermore, both figures show that, a significant coupling between both inputs and outputs. Because of that, the controller is to achieve faster response, robust and disturbance recovery, less interactions, and with minimum energy which will be presented in the chapter IV.

### **3.3.Least Effort Regulation Configuration.**

This new control method is split into two loops, outer and inner, the inner loop works as a regulator to maintain the system stability, on the other hand, the outer loop helps in suppress the disturbance on the system. The following derivation is a rewriting for Whalley and Ebrahimi (2006).

In the frequency domain, the Laplace representation of the system model is written as:

$$y(s) = G(s)u(s) + \delta(s) \quad 3-10$$

The control law of the inner loop is as per the following:

$$k(s)[\bar{r}(s) - h(s)y(s)] \quad 3-11$$

Which will satisfy the desired system behavior in terms of stability, when  $k(s)$  and  $h(s)$  designed carefully.

On the other hand, the outer loop control law will be as the following:

$$P(r(s) - Fy(s)) \quad 3-12$$

Where P and F are designed values to ensure the system decoupling and disturbance rejection.

Consequently, the completed control law for the inner and outer loops can be written as:

$$u(s) = k(s)[\bar{r}(s) - h(s)y(s)] + P(r(s) - Fy(s)) \quad 3-13$$

Where  $F = \text{Diag}(f_j, f_j, \dots, f_j)$ ,  $0 < f_j < 1$

And assuming that  $\bar{r}(s) = 0$

The closed loop response for the system model with the controller (inner and outer loops) is:

$$y(s) = (I_m + G(s)(k(s) >< h(s) + PF))^{-1} x(G(s)Pr(s) + \delta(s)) \quad 3-14$$

Taking into consideration that

$$\| | G(s)(k(s) >< h(s) + PF) | |_{\infty}$$

Is finite for all s on the D contour.

And by choosing the steady state matrix  $S_s$  to satisfy that  $y(0) = S_s r(0)$  and assuming  $\delta(s)$  is null.

$$P = (G(0)^{-1} + k(0) \gg h(0)) S_s (I - FS_s)^{-1} \quad 3-15$$

For the sake of decoupling the steady state response,  $S_s = I_m$  where  $I_m$  is the identity matrix of  $m \times m$  size. Or, in order to achieve low steady state interaction  $S_s$  diagonal elements to be of unity value while the off diagonal elements to be  $|s_{i,j}| \ll 1$ .

Applying the above, the output response would be:

$$y(s) = \{(I_m + G(s)[k(s) \gg h(s) + (G(0)^{-1} + k(s) \gg h(s))(I_m - F)^{-1}F]\}^{-1} \{(G(s)Pr(s) + \delta(s))\} \quad 3-16$$

At low frequencies when  $G(s) \cong G(0)$  and  $G(s)G(0)^{-1} \cong I_m$

$y(s)$  would be in the following form:

$$\cong \{[I_m + G(s)k \gg h(s)][I_m + (I_m - F)^{-1}F]\}^{-1} \{G(s)Pr(s) + \delta(s)\}$$

If the elements of the F matrix is  $0 < f_m < 1$  then the output would be in simpler form of:

$$\cong (1 - f)[I_m + G(s)k \gg h(s)]^{-1} \{G(s)Pr(s) + \delta(s)\} \quad 3-17$$

Then at low frequencies and as:

$$G(s)P = G(s)[G(0)^{-1} + k(0) \gg h(0)][(I_m - F)^{-1}] \quad 3-18$$

Finally the output response at the low frequencies would be in the following form:

$$y(s) = I_m r(s) + S(s)\delta(s) \quad 3-19$$

where  $S(s)$  the sensitivity matrix at low frequencies is:

$$S(s) = (1 - f)(I_m + G(s)k(s) \gg h(s))^{-1} \quad 3-20$$

Obviously, the steady state non interaction will be achieved regardless of the changes in the reference input  $r(s)$ . Otherwise referring to the sensitivity matrix it is shown that by increasing the value of  $f$  but not exceeding the unity there will be more disturbance rejection.

In the sight of the above, the design methodology here is to alter the  $k(s)$  and  $h(s)$  in order to achieve the desired system dynamics. On the other hand and in order to achieve the steady state decoupling and disturbance rejection a pre-compensator  $P$  to be configured with careful choosing of the  $f$  feedback gain. The following paragraphs show the design strategy for altering the inner loop vectors  $k(s)$  and  $h(s)$  and configuring the pre compensator  $P$ .

### Inner loop analysis:

By considering the system transfer function  $G(s)$  is square with dimension  $m \times m$ , linear, regular, proper or strictly proper and it can be factorized as:

$$G(s) = L(s) \frac{A(s)}{d(s)} R(s) \text{ Assuming no time delay.}$$

Where

$$L(s) = \text{Diag} \left( \frac{\gamma_j(s)}{p_j(s)} \right) \text{ contains the left row factors}$$

$$R(s) = \text{Diag} \left( \frac{\rho_j(s)}{q_j(s)} \right) \text{ contains the right column factors.}$$

$$\text{and } \frac{A(s)}{d(s)} \in H_\infty.$$

$A(s)$  is a non-singular matrix of rational functions where  $\det A(s) \neq 0$ .

$$\text{and } d(s) = s^k + a_1 s^{k-1} + \dots + a_0.$$

Since the output response is:

$$y(s) = G(s)u(s) + \delta(s)$$

If the control satisfies the following:

$$u(s) = k(s)[\dot{r}(s) - h(s)y(s)]$$

The equations of the output and the input could be combined in the following:

$$y(s) = (I_m + G(s)k(s) \succ \langle h(s))^{-1} (G(s)k(s)\dot{r}(s) + \delta(s)) \quad 3-21$$

If  $k(s)$  is a result of  $k\phi_j(s)$  and  $h(s) = hX_j(s)$ .

Where  $k$  and  $h$  are vectors,  $\phi_j(s)$  and  $X_j(s)$  are proper or strictly proper, stable and minimum phase functions then they may be chosen such that:

$$y(s) = \left( I_m + L(s) \frac{A(s)}{d(s)} R(s)k(s) \succ \langle h(s) \right)^{-1} * (L(s) \frac{A(s)}{d(s)} R(s)k(s)\dot{r}(s) + \delta(s)) \quad 3-22$$

The determinant required in the above equation is:

$$\det [ I_m + L(s) \frac{A(s)}{d(s)} R(s)k(s) \succ \langle h(s) ] = 1 + \langle h \frac{A(s)}{d(s)} k \rangle. \quad 3-23$$

The inner product in the above equation may be represented as

$$\langle h(s) \frac{A(s)}{d(s)} k \rangle = [1, s, \dots, s^{m-1}] * \begin{bmatrix} \gamma_{11} & \dots & \gamma_{mm} \\ \vdots & \ddots & \vdots \\ b_{11} & \dots & b_{mm} \\ a_{11} & \dots & a_{mm} \end{bmatrix} * \begin{bmatrix} k_1 h_1 \\ k_2 h_1 \\ \cdot \\ k_m h_m \end{bmatrix} \quad 3-24$$

If the gain ratios  $n$  satisfying

$$k_2 = n_1 k_1, k_3 = n_2 k_1 \dots k_m = n_{m-1} k_1$$

$$\text{and } < hA(s)k \geq b(s) \quad 3-25$$

Consequently,

$$k_1[Q]h = (b_{m-1}, b_{m-2}, \dots, b_0)^T \quad 3-26$$

Where Q is

$$\begin{bmatrix} \gamma_{11} + \gamma_{12}n_1 + \gamma_{1m}n_{m-1} & \vdots & \gamma_{21} + \gamma_{22}n_1 + \gamma_{2m}n_{m-1} & \vdots & \cdots & \gamma_{m1} + \gamma_{m2}n_1 + \gamma_{mm}n_{m-1} \\ & \vdots & & \vdots & & \vdots \\ b_{11} + b_{12}n_1 + b_{1m}n_{m-1} & \vdots & b_{21} + b_{22}n_1 + b_{2m}n_{m-1} & \vdots & \cdots & b_{m1} + b_{m2}n_1 + b_{mm}n_{m-1} \\ a_{11} + a_{12}n_1 + a_{1m}n_{m-1} & \vdots & a_{21} + a_{22}n_1 + a_{2m}n_{m-1} & \vdots & \cdots & a_{m1} + a_{m2}n_1 + a_{mm}n_{m-1} \end{bmatrix}$$

By choosing a suitable  $b(s)$  function by any method, the gain ratio can be calculated. Then, the vector  $h$  can be calculated based on the arbitrary selection of  $k_1$ .

In view of the above, and in order to optimize the effort of the controller, achieving the disturbance rejection and maintaining the inner loop dynamics, the control effort function must be defined and methodology for choosing the gain ratios must be adopted.

The controller effort in time domain is proportional to:

$$\begin{aligned} & (|k_1h_1| + |k_2h_1| + \cdots |k_mh_1|)|y_1(t)| + (|k_1h_2| + |k_2h_2| + \cdots |k_mh_2|)|y_2(t)| + \cdots \\ & + (|k_1h_m| + |k_2h_m| + \cdots |k_mh_m|)|y_m(t)| \end{aligned}$$

So, the costs of control energy is proportionally related to:

$$E(t) = \int_{t=0}^{t=T_f} (\sum_{i=1}^m k_i^2 \sum_{j=1}^m h_j^2 y_j^2(t)) dt \quad 3-27$$

which leads to the following control index:

$$J = \sum_{i=1}^m k_i^2 \sum_{j=1}^m h_j^2$$

which minimizing it means minimizing the required control effort.

If

$$k_2 = n_1 k_1, k_3 = n_2 k_1 \dots k_m = n_{m-1} k_1$$

Then J can be rewritten as:

$$J = (k_1)^2 (1 + n_1^2 + n_2^2 + \dots + n_{m-1}^2) (h_1^2 + h_2^2 + \dots + h_m^2) \quad 3-28$$

where  $(h_1^2 + h_2^2 + \dots + h_m^2) < h, h >$ .

From the determinant of equation (3-23) and inner product in equation (3-24) and in light of equation (3-26), h can be rewritten as:

$$h = k_1^{-1} Q^{-1} b \quad 3-29$$

Then equation (3-28) becomes in the following format:

$$J = (1 + n_1^2 + n_2^2 + \dots + n_{m-1}^2) b^T (Q^{-1})^T Q^{-1} b$$

With m depending on the system, for 2x2 system, m=2:

$$J = (1 + n_1^2) b^T (Q^{-1})^T Q^{-1} b \quad 3-30$$

To minimize J, differentiation to base  $n_1$  is applied,

$$\frac{\partial J}{\partial n_1} = 0$$

Which finds the value minimizing the J.

Which achieves the inner loop desired performance.

Although of the above, this achievement is still not sufficient for disturbance suppression and then recovery of the system.

In order to achieve the steady state and disturbance rejection conditions, the feedback gain of the outer-loop could be adjusted between the values 0 and 1. Which alters the system transient response, the optimum  $f$  value should be chosen by examining the transient response.

Referring to equation (3-14) and to combine the two loops (inner and outer), the denominator of equation (3-14) is the base of the stability condition.

For analysis purpose, if  $f_1, f_2, \dots, f_m = f$ , then equation(3-14) denominator can be calculated from:

$$\det\{I_m + G(s) \left( \frac{k(s) \gg h(s)}{(1-f)} \right) + \left( \frac{G(0)^{-1} f}{(1-f)} \right)\} \quad 3-31$$

It is clear from the function  $1 - f$  that, as  $f \rightarrow 1$ , the feedback compensator matrix

$\left[ \left( \frac{k(s) \gg h(s)}{(1-f)} \right) + \left( \frac{G(0)^{-1} f}{(1-f)} \right) \right]$  goes to infinity which leads to system instability.

On the other hand, two ranges of  $f$  values can be identified as per the following:

- $0 < f \leq 0.5$ , these range of values have amplification effect on the inner loop feedback gain. In contrast, attenuation effect on the outer loop. These two effects occurred as a result of  $\frac{G(0)^{-1} f}{(1-f)}$ .
- $0.5 < f < 1$ , leads to amplification of the inner and outer loop gains, which is a result of  $\frac{f}{1-f}$  and  $\frac{1}{1-f}$ .

Consequently, the initial minimum value of  $J$  is increased after increasing the values of  $f$  but with no effect on the gain ratio  $n$ . in light of the above, the steady state and transient disturbance rejection and recovery is achieved.

### 3.4.H-infinity Method.

The H infinity controller is a controller proposed by Zames, using the mathematical optimization as a way to find a feedback which satisfies the desired optimization. The  $H^\infty$  Loop Shaping provides a mechanism to balance robust stability requirements with the disturbance rejection specifications (McFarlane and Glover, 1992).

Figure 3-5, depicts the block diagram of general plant model of the transfer function matrix  $G(s)$  controlled by matrix  $K(s)$ . Where  $w$  is the vector of disturbance signals,  $z$  is the cost signals consisting of all errors,  $v$  is the vector consisting of measurement variables and  $u$  is the vector of all control variables.

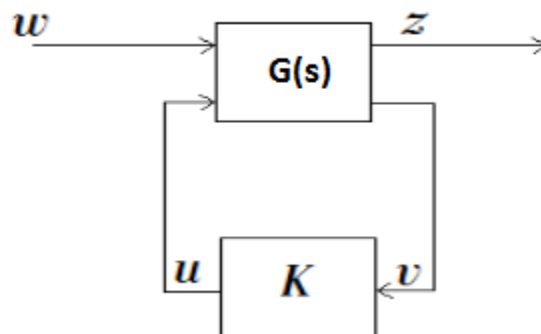


Figure 3-5, Control system diagram.

From the above, the nominal plant  $G(s)$  can be split as following:

$$G(s) \begin{bmatrix} G_{11}(s) & G_{12}(s) \\ G_{21}(s) & G_{22}(s) \end{bmatrix}$$

So,

$$z = G_{11}w + G_{12}u \text{ and } y = G_{21}w + G_{22}u$$

Considering the feedback law,  $u = K(s)y$  and applying substitutions on the above equations:

$$z = [G_{11} + G_{12}K(I - G_{22}K)^{-1}G_{21}]w \quad 3-32$$

$[G_{11} + G_{12}K(I - G_{22}K)^{-1}G_{21}]$  can be denoted by  $F_1(G, K)$

$$\text{So, } z = F_1(G, K)w$$

Consequently, to minimize the error signal  $z$  due to  $w$ ,  $F_1(G, K)$  must be minimized.

$$\begin{bmatrix} z_1 \\ z_2 \\ z_3 \\ e \end{bmatrix} = \begin{bmatrix} W_1 & W_1G \\ 0 & W_2 \\ 0 & W_3G \\ I & -G \end{bmatrix} \begin{bmatrix} w \\ z \end{bmatrix} \quad 3-33$$

The objective here is to find the controller  $K(s)$ , which uses the information in  $v$ , to generate control signals  $u$  which responds to the effect of  $w$  on  $z$ .

In order to design the  $H_\infty$  robust controller, three criteria must be defined:

1. Performance criteria: by verifying that, the sensitivity function  $S(s) = [I + G(s)K(s)]^{-1}$  is small for all range of frequencies where the disturbance inputs are large.
2. To limit the noise effect, the closed loop transfer function must be kept small at high frequencies, (i.e minimise  $T(s) = I - S(s)$ , as  $w \rightarrow \infty$ ).
3. Robustness criteria: The maintaining of the stability even with existence of parameters variation by minimizing  $K[I + G(s)K(s)]^{-1}$ .

Consequently, the  $H_\infty$  problem can be summarised in minimizing the following function:

$$F_1(G, K) = \begin{bmatrix} W_1 S \\ W_2 R \\ W_3 T \end{bmatrix} \text{ where } W_1, W_2 \text{ and } W_3 \text{ are frequency dependent matrices.}$$

Before getting to the controller design the norm must be defined.

The  **$H_\infty$  norm** is the maximum singular value of a transfer function  $G$  over the complete spectrum which is expressed as:

$$\|G(j\omega)\|_\infty = \sup \sigma(G(j\omega)) \text{ where } \sigma \text{ is the maximum singular value, Figure 3-6.}$$

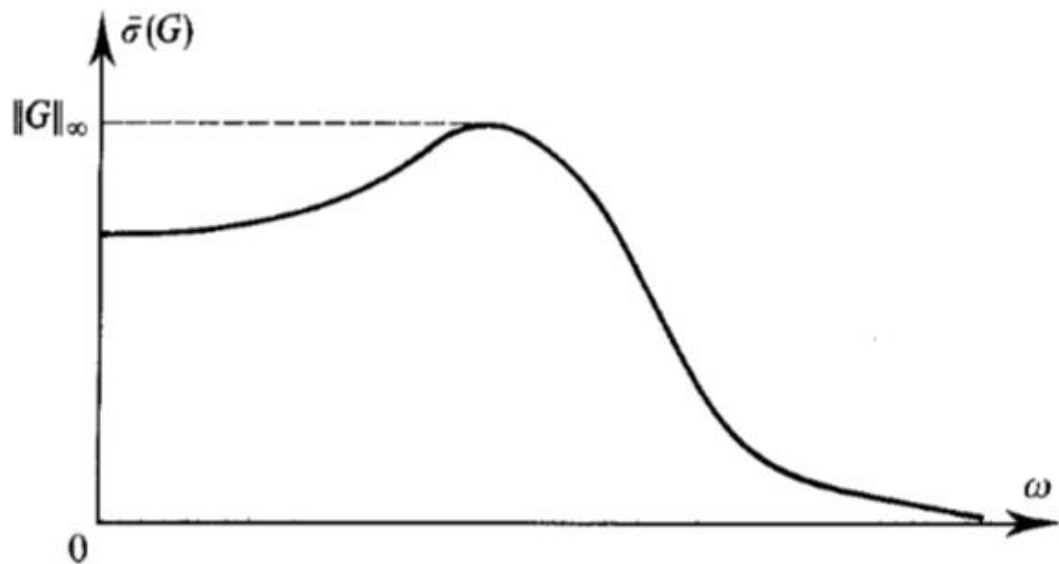


**Figure 3-6**, Reading off  $\|G\|_\infty$  from plot of largest principal gain (Maciejowski, 1996)

So, the aim now is to design a controller  $K(s)$  which minimises the  $H_\infty$  norm of the closed loop transfer function. This can be achieved by using weighting functions  $W_1, W_2$  and  $W_3$  which limit the error signal, the control signal, and the output signal, Figure 3-7.

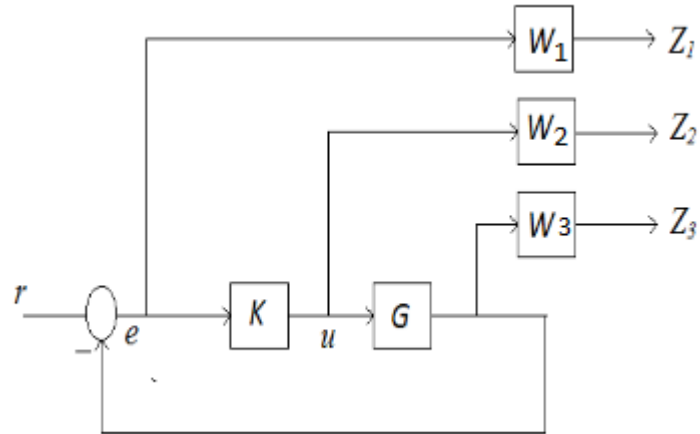


**Figure 3-7, The  $H^\infty$  Framework.**

These weighting functions are based on the sensitivity function, the control function and the complementary sensitivity function, which are represented respectively by:

$$S = [I + K(s)G(s)]^{-1} \quad 3-34$$

$$R = K[I + K(s)G(s)]^{-1} \quad 3-35$$

$$T = K(s)G(s)[I + K(s)G(s)]^{-1} \quad 3-36$$

the using of the above mentioned functions with the weighting functions must meet the following constraints:

$$\| |W_1 S| | \|_\infty \leq \gamma \approx 1$$

$$\| |W_2 R| | \|_\infty \leq \gamma \approx 1$$

$$\| |W_3 T| | \|_\infty \leq \gamma \approx 1$$

which is called mixed sensitivity problem which is considered a special case of the H-infinity method (Verma & Jonckheere 1984).

Besides that, those weighting functions help to allow an exact frequency domain loop shaping. This means that the controller shapes the signals to the inverse of the weighting functions. And, the plant will be augmented taking the following expression:

$$\begin{bmatrix} z_1 \\ z_2 \\ z_3 \\ e \end{bmatrix} = \begin{bmatrix} W_1 & W_1 G \\ 0 & W_2 \\ 0 & W_3 G \\ I & -G \end{bmatrix} \begin{bmatrix} w \\ z \end{bmatrix} \quad 3-37$$

### **General guidelines for weights selection:**

The following lines includes a selection of weighting functions, for the sensitivity function, complementary sensitivity function and the control weights. The weighting function for the sensitivity function is chosen to show the desired system dynamics. In a way to maintain the low gain at low frequencies for good tracking performance and high gain at high frequencies to limit the overshooting. ( John E. Bibel and D. Stephen Malyevac, 1992).

On the other hand, the complementary sensitivity function is weighted to make the system insensitive to noise which achieves the robustness properties. Since the noise occurs at high frequencies comparing to the control input, a high pass filter is used for this purpose.

In addition, weighting functions can have high orders which is more flexible and easier in achieving the desired characteristics of the system. But, higher orders of weighting functions reflects in higher order of the controller, which is equal to the order of the nominal plant plus the weights orders.

## Chapter IV:

### 4. Simulation Results and Discussions

#### 4.1. Least Effort Regulation.

Referring to the methodology represented in the previous chapter, an application to the wind turbine model will be discussed here.

The transfer function representing the wind turbine model is:

$$G(s) = \begin{bmatrix} \frac{-70.55}{15s+0.233} & \frac{-1.56}{30s^3+15.47s^2+2.48s+0.035} \\ \frac{3458s+173.1}{15s+0.233} & \frac{-8.05}{30s^3+15.47s^2+2.48s+0.035} \end{bmatrix} \quad 4-1$$

Before using the least effort theory, the open loop transfer function must be put in the form of the following equation:

$$G(s) = L(s) \frac{A(s)}{d(s)} R(s) \Gamma(s) \quad 4-2$$

For doing that, the model should be multiplied by a suitable matrix (pre-compensator) results in a common denominator for all transfer function elements. In order to select that matrix a factorization to the transfer function denominator of column two and dividing both denominators and numerators by the common factor in each column is done which leads to the transfer function arrangement of equation:

$$G(s) = \begin{bmatrix} \frac{-4.7}{s+0.016} & \frac{-0.052}{(s+0.016)(s^2+0.5s+0.075)} \\ \frac{230.53s+11.54}{s+0.016} & \frac{-0.268}{(s+0.016)(s^2+0.5s+0.075)} \end{bmatrix} \quad 4-3$$

Looking at the factorized model, the pre-compensator

$$K(s) = \begin{bmatrix} \frac{1}{s^2+0.5s+0.075} & 0 \\ 0 & 1 \end{bmatrix} \text{ could be used since it doesn't affect the stability of the open loop}$$

system and achieve the desired format of equation(4-2).

By multiplying the pre-compensator with the model transfer function, this yields to the desired format:

$$\begin{aligned} G(s) &= \begin{bmatrix} \frac{-4.7}{(s+0.016)(s^2+0.5s+0.075)} & \frac{-0.052}{(s+0.016)(s^2+0.5s+0.075)} \\ \frac{230.53s+11.54}{(s+0.016)(s^2+0.5s+0.075)} & \frac{-0.268}{(s+0.016)(s^2+0.5s+0.075)} \end{bmatrix} \\ &= \begin{bmatrix} \frac{-4.7}{(s^3+0.516s^2+0.083s+0.001)} & \frac{-0.052}{(s^3+0.516s^2+0.083s+0.001)} \\ \frac{230.53s+11.54}{(s^3+0.516s^2+0.083s+0.001)} & \frac{-0.268}{(s^3+0.516s^2+0.083s+0.001)} \end{bmatrix} \end{aligned}$$

Since,  $L(s) = I_2$ ,  $\Gamma(s) = I_2$  and  $R(s) = I_2$ . So,

$$\frac{A(s)}{d(s)} = \begin{bmatrix} \frac{-4.7}{(s+0.016)(s^2+0.5s+0.075)} & \frac{-0.052}{(s+0.016)(s^2+0.5s+0.075)} \\ \frac{230.53s+11.54}{(s+0.016)(s^2+0.5s+0.075)} & \frac{-0.268}{(s+0.016)(s^2+0.5s+0.075)} \end{bmatrix} \quad 4-4$$

So the rational matrix A(s) is:

$$A(s) = \begin{bmatrix} -4.7 & -0.052 \\ 230.53(s+0.05) & -0.268 \end{bmatrix}$$

And  $d(s)$  is:

$$d(s) = (s + 0.016)(s^2 + 0.5s + 0.075)$$

According to equation (3-24):

$$\begin{aligned} \langle h(s)A(s)k \rangle &= [h_1, h_2] * \begin{bmatrix} -4.7 & -0.052 \\ 230.53(s + 0.05) & -0.2683 \end{bmatrix} \begin{bmatrix} k_1 \\ k_2 \end{bmatrix} \\ &= (-4.7k_1h_1 - 0.052k_2h_1 + 230.53(s + 0.05)k_1h_2 - 0.2683k_2h_2) \\ &= [1 \quad s] \begin{bmatrix} -4.7 & -0.052 & 11.54 & -0.2683 \\ 0 & 0 & 230.53 & 0 \end{bmatrix} \begin{bmatrix} k_1h_1 \\ k_2h_1 \\ k_1h_2 \\ k_2h_2 \end{bmatrix} \end{aligned}$$

the gain ratio  $n$ , where  $k_2 = nk_1$  is substituted to result in matrix  $Q$ :

$$= \begin{bmatrix} -4.7 - 0.052n & 11.53 - 0.2683n \\ 0 & 230.53 \end{bmatrix}$$

In order to enhance the system dynamics, an inner loop regulator will be designed based on an equivalent single transfer function to the multivariable system. According to the following equation:

$$\langle h \frac{A(s)}{d(s)} k \rangle = \frac{b(s)}{d(s)}$$

where  $d(s) = (s + 0.016)(s^2 + 0.5s + 0.075)$ , which gives the system poles  $s = -0.25 - 0.11i$ ,  $s = -0.25 + 0.11i$  and  $s = -0.016$ . The slowest pole is  $-0.016$  which is nearer to the imaginary axis. Assume  $b(s) = b_0(s + 0.016)$ , the slowest system poles will be cancelled which leads the system to be identical second order system which has a faster response.

The root locus of:

$$\frac{b(s)}{d(s)} = \frac{b_0(s + 0.016)}{(s + 0.016)(s^2 + 0.5s + 0.075)}$$

$$-1 = \frac{b_0}{(s^2 + 0.5s + 0.075)} \quad 4-5$$

is depicted in Figure 4-1:

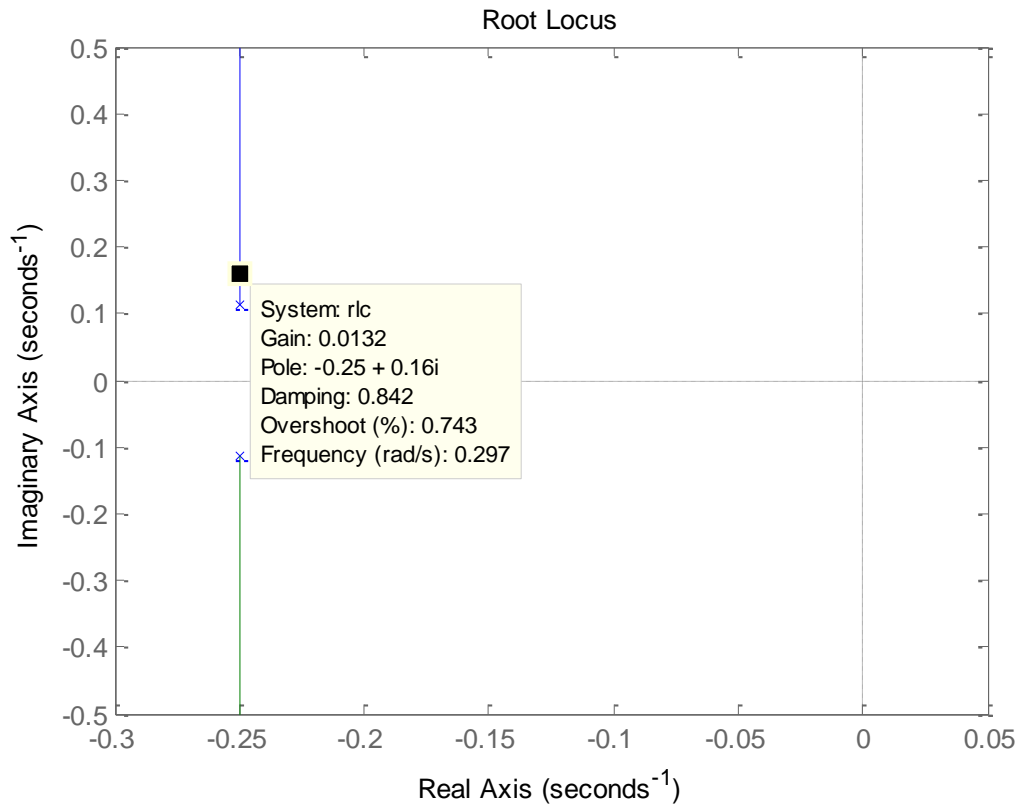


**Figure 4-1**, Root Locus of equation (4-5)

Consequently, gain  $b_0 = 0.013$  is chosen to achieve the desired system dynamics. Now using this equation  $k_1[Q]h = b(s)$  and substituting  $Q$ ,  $b = b_0 \begin{bmatrix} 0.016 \\ 1 \end{bmatrix} = \begin{bmatrix} 0.0002 \\ 0.013 \end{bmatrix}$  and assuming  $k_1 = 1$  the inner loop feedback gain values will be:

$$h = \frac{Q^{-1}b}{k_1} = [9.4 * 10^{-5} \quad 5.6 * 10^{-5}]$$

In order to complete the design for the inner loop a value of  $k_2$  should be found. For that, the performance index equation (4-6) will be used to give the optimum gain ratio value  $n$  which leads to the minimum controller effort.

The performance index equation is:

$$J = (1 + n^2)b^T(Q^{-1})^T Q^{-1}b \quad 4-6$$

Referring to the previous root locus Figure 4-1 and  $b$  along with substitution of  $Q$  matrix, the performance index equation can be written as:

$$J \cong \frac{1.968 * 10^9 n^4 - 9.8 * 10^{10} n^3 + 2.2 * 10^{12} n^2 - 9.8 * 10^{10} n + 2.2 * 10^{12}}{22 * 10^{15} n^2 + 4 * 10^{18} n + 1.8 * 10^8}$$

Based on the previous equation and as depicted in Figure 4-2, the optimum performance index can be found after by finding  $n$  values of  $\frac{\partial j}{\partial n} = 0$ .

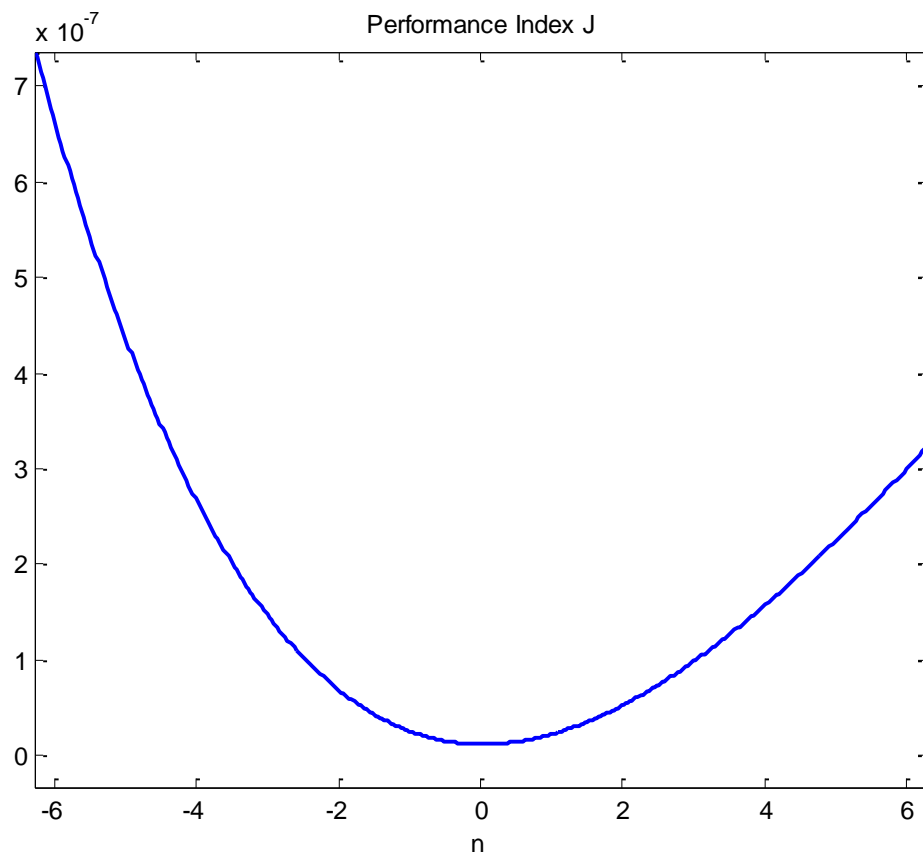


**Figure 4-2**, Performance Index J.

Which gives the following  $n$  values:

$n = 0.0333$  where  $j = 1.2 * 10^{-8}$  (Minimum).

$n = -193.48$  where  $j = 0.0149$  (Maximum)

$n = 1.287 * 10^{-6} \pm 8.14 * 10^{-7}$  (Not real number)

Consequently,  $n = 0.0333$  is selected as a gain ratio to be implemented in the inner loop controller which results in feed forward gain values  $k = \begin{bmatrix} 1 \\ 0.0333 \end{bmatrix}$ .

Moreover and for designing the gains of feedforward and feedback outer loop controller, computations is remaining, which is in the following lines:

Since  $G(s) = \langle h \frac{A(s)}{d(s)} k \rangle$ ,  $k = \begin{bmatrix} 1 \\ 0.0333 \end{bmatrix}$ ,  $h = [9.4 * 10^{-5} \quad 5.6 * 10^{-5}]$  and the steady state value of the model transfer function is given by:

$$G(0) = \begin{bmatrix} -4700 & -52 \\ 11540 & -268.3 \end{bmatrix}$$

Moreover and due to the design requirements for limiting the steady state interaction in the closed loop response to a peak point of 10%, a steady state matrix is assumed to be

$$S_s \begin{bmatrix} 1 & 0.1 \\ 0.1 & 1 \end{bmatrix}.$$

Following that, the outer loop feedback gains must be selected between values of  $0 < f < 1$ .

Since  $f$  is range of values, an examination of some values will be studied taking into considerations how an increasing of  $f$  will have a significant effect on the closed loop response, particularly the disturbance rejection.

First, the feedback values of  $f$  for the two outputs rotor speed and generated power is

represented by the matrix  $F = \begin{bmatrix} f_1 & 0 \\ 0 & f_2 \end{bmatrix}$ .

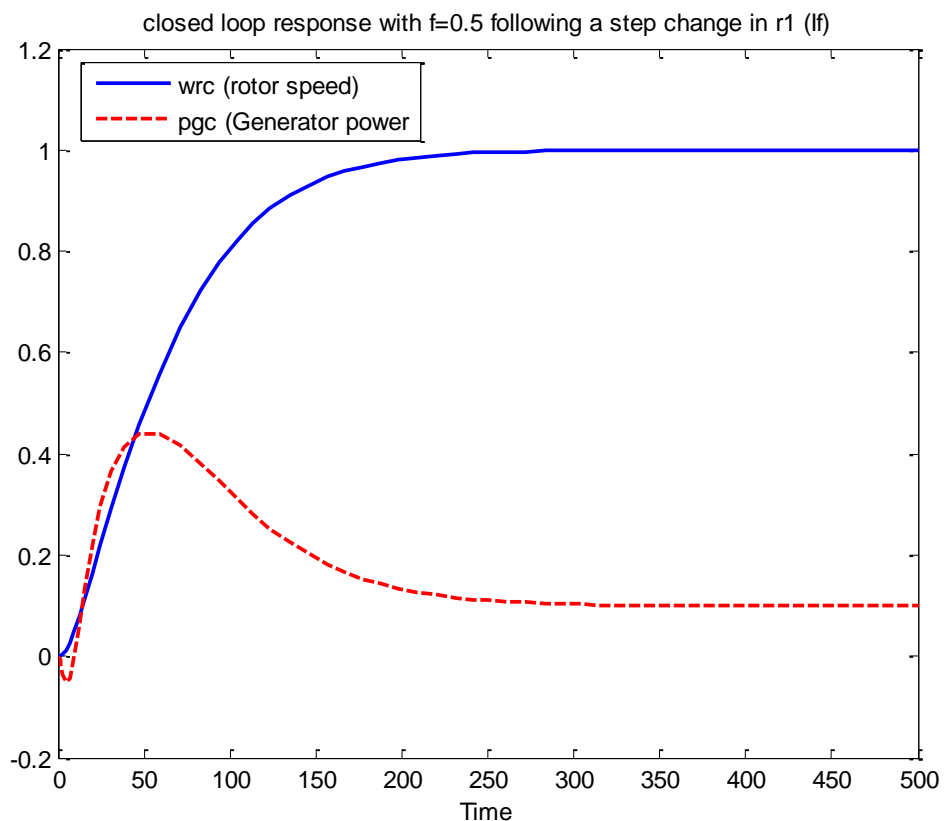
Assuming that  $F = \begin{bmatrix} 0.5 & 0 \\ 0 & 0.5 \end{bmatrix}$  and referring to the equation (3-15), this leads to an outer loop

feedforward gain values of  $P = \begin{bmatrix} -0.000068 & 0.000152 \\ -0.013665 & -0.007653 \end{bmatrix}$

Substituting the resulted gain values in the simulation model represented by MATLAB SIMULINK shown in Figure A-1 (Appendix).

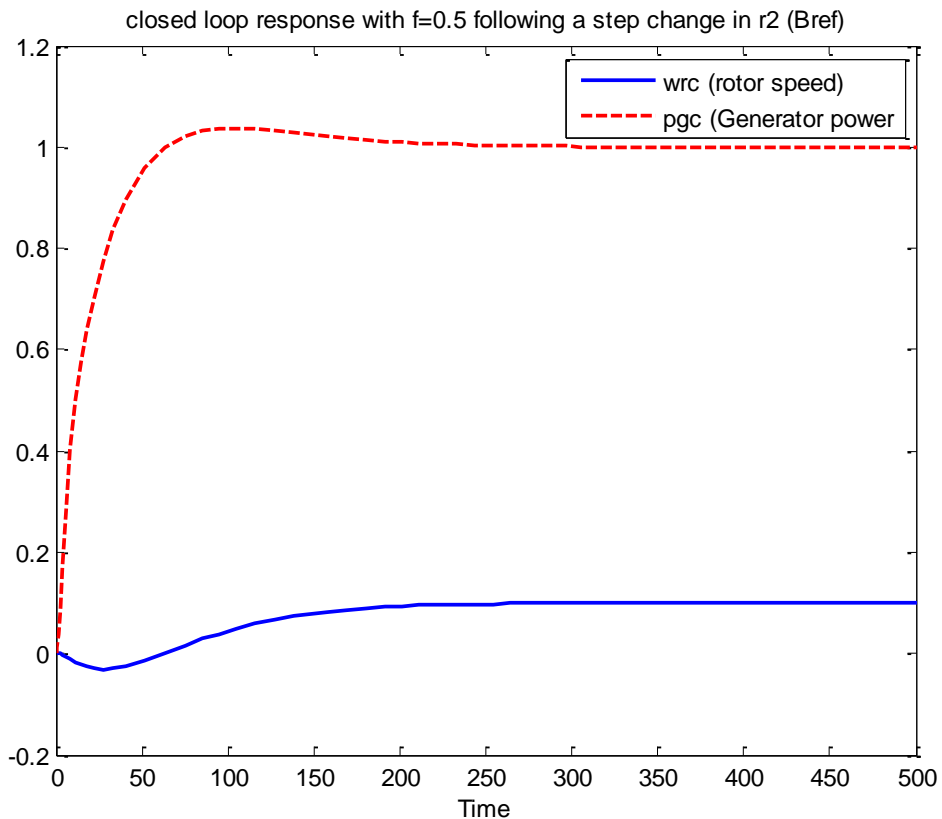
The model is first simulated by applying a unit step change in the reference inputs, first input is the field current  $I_f$  and the second one is the reference pitch angle  $B_{ref}$ , respectively.

Figure 4-3 depicts the response following a unit step change in the first input  $I_f$ , the output response of the closed loop with  $f_{1,2} = 0.5$  is good but not the desired one.



**Figure 4-3,** Closed Loop response with  $f=0.5$  following a step change in  $r1$  ( $I_f$ )

The response is stable and it can be noticed that, both output responses settling time has improved which is less than 250 seconds. While the first output response (rotor speed) has a rising time which is around 150 seconds. The second output response (Generator power) has inadequate overshooting exceeds 200% of the steady state output . That is because of the zero in the transfer function element  $g_{21}$  which is  $\frac{230.53s+11.54}{(s+0.016)(s^2+0.5s+0.075)}$  which increases the overshooting, decreases the rise time. Additionally, no interaction is noticed between the two outputs. Both outputs settled on 1 and 0.1 as set in the steady state matrix  $S_s$ . On the contrary, Figure 4-4 shows the response following a unit step change in the second input  $B_{ref}$  with the same value of  $f_{1,2} = 0.5$ .



**Figure 4-4**, Closed Loop response with  $f=0.5$  following a step change in  $r_2$  ( $B_{ref}$ )

It can be noticed that, the first output is overdamped with settling time of less than 200 seconds and of a 10 percent of the value of the second output in the steady state mode as desired. On contrast, the second output has a slight overshooting with settling time less than 200 seconds which is an improvement in comparison with open loop response as previously shown in Figure 3-4 in chapter three.

By choosing  $F = \begin{bmatrix} 0.7 & 0 \\ 0 & 0.7 \end{bmatrix}$ , the closed loop response of unit step changes in first input  $I_f$  and the second input  $B_{ref}$  is simulated respectively. As shown in Figure 4-5 , the response is faster with settling time less than 150 seconds for both outputs. On the other hand,

the second output has negligible overshooting. And alike when  $f$  was 0.5, no interaction is noticed.

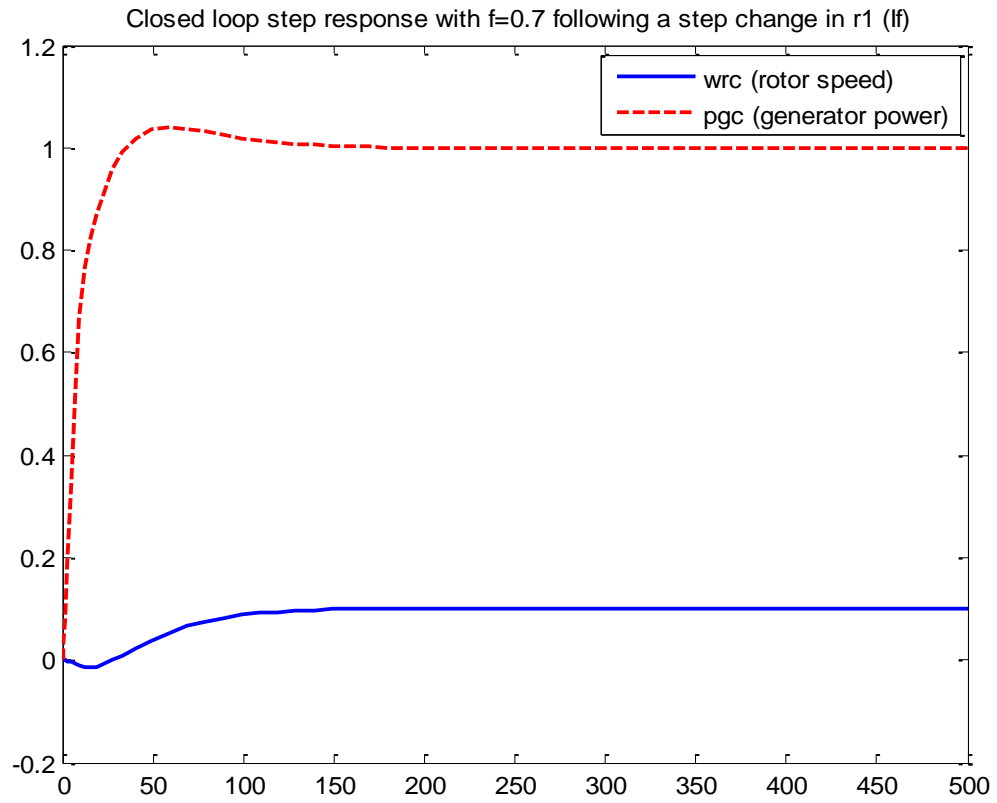


**Figure 4-5,** Closed Loop response with  $f=0.7$  following a step change in  $r1$  (If)

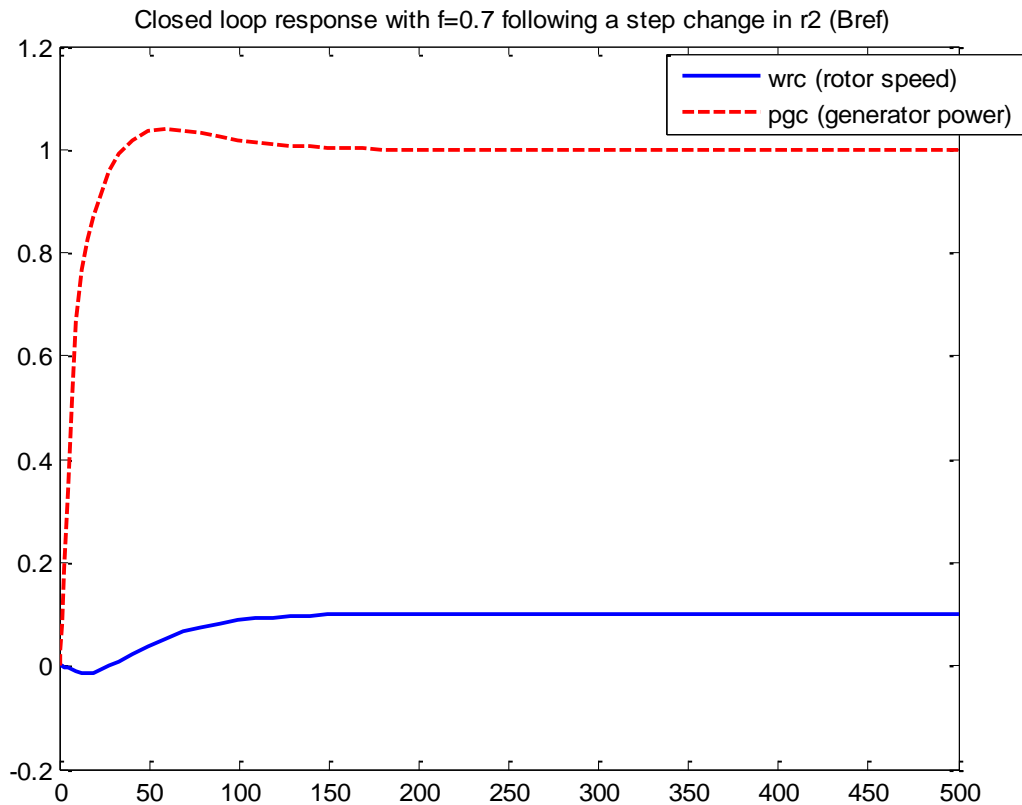


**Figure 4-6**, Closed Loop response with  $f=0.7$  following a step change in  $r_2$  (Bref)

For further analysis, feedback matrix is chosen to be  $F = \begin{bmatrix} 0.8 & 0 \\ 0 & 0.8 \end{bmatrix}$  and consequently the feedforward gain matrix became  $P = \begin{bmatrix} -0.000060 & 0.000373 \\ -0.045876 & -0.034066 \end{bmatrix}$ . Increasing the feedback matrix  $F$  leads to increasing in the feedforward gain matrix which has a clear effect on the output overshooting particularly for the second output (generated power) whether there was a step change in the field current ( $r_1$ ) or the change was in the pitch angle ( $r_2$ ), Figure 4-7 and Figure 4-8, respectively.

In spite of that, the tremendous improvement in the speed of response cannot be neglected. Applying a step change in the field current, the rise time of the rotor speed is less than 50s and settling time of less than 100s. On the other output, it is depicted that, a radical overshooting has taken place in the generated power but with a significant decreasing in settling time of less than 100 seconds.

However, and from all the above it can be noticed the improvements in the speed of the response and the outputs non-interaction of both outputs.

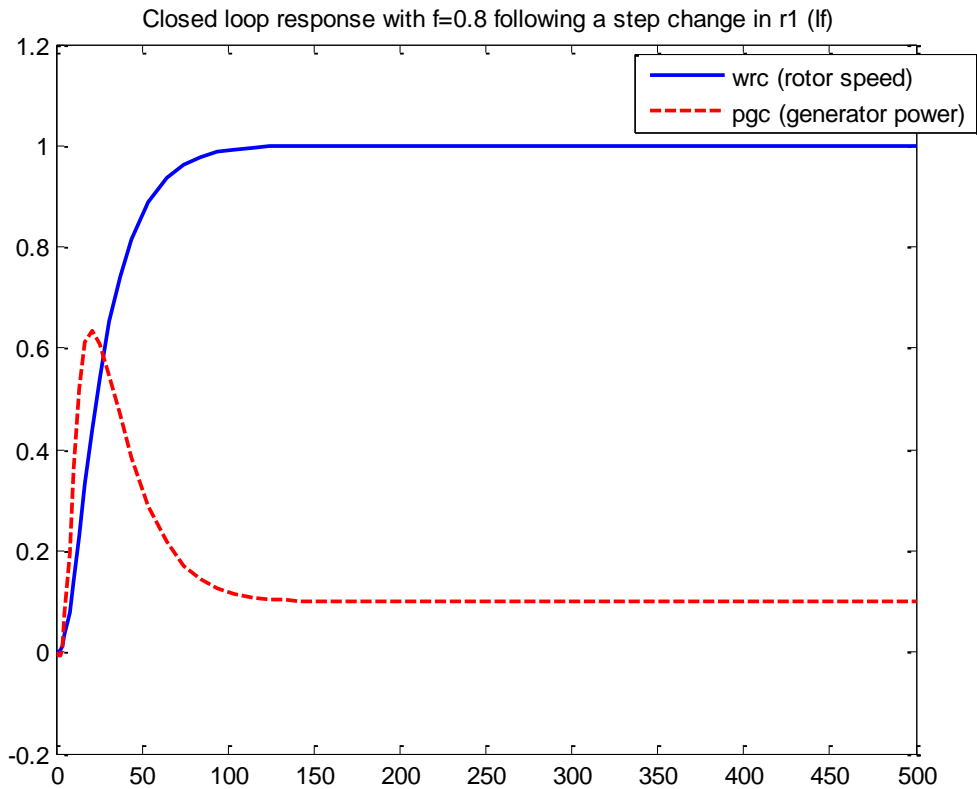


**Figure 4-7**, Closed Loop response with  $f=0.8$  following a step change in  $r1$  (If)

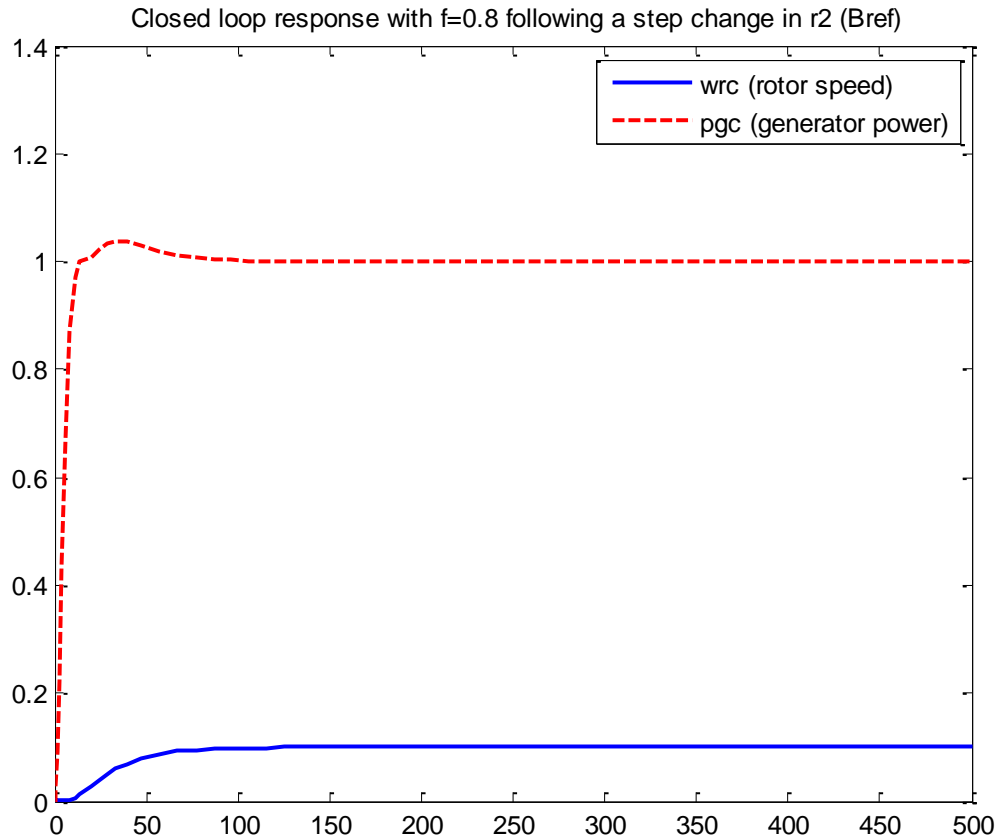


**Figure 4-8,** Closed Loop response with  $f=0.8$  following a step change in  $r_2$  (Bref)

In order to inspect the robustness of the controller and its response to the disturbances, a disturbance in form of unit step is applied on the first output. The closed loop response is simulated for different  $F$  values which is depicted in Figure 4-9.

It is very clear that how the system is improving by increasing the values of  $f_{1,2}$  from 0.5 to 0.8 where the recovery from disturbance is the highest and fastest when  $f_{1,2}$  is 0.8.

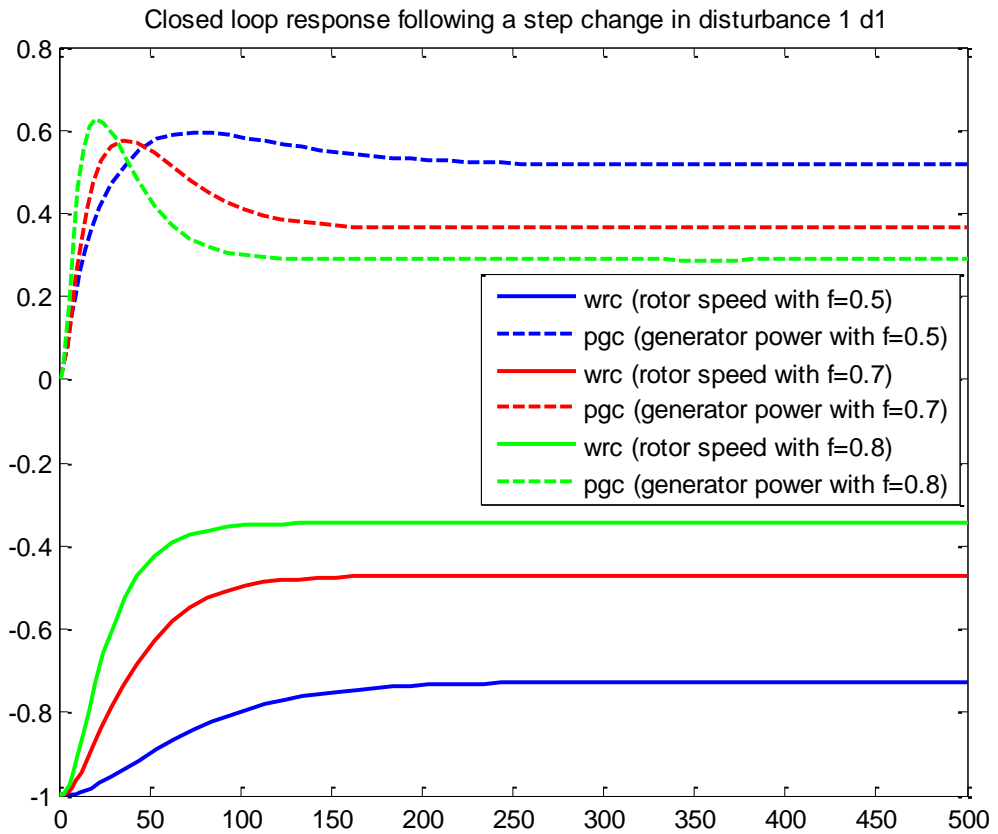


**Figure 4-9**, Closed Loop response following a step change in disturbance  $d_1$

Which is the same case in applying a step unit disturbance on output 2 (the Generated Power) with faster recovery time when  $f_{1,2}$  is 0.8 and higher rejection, Figure 4-10.

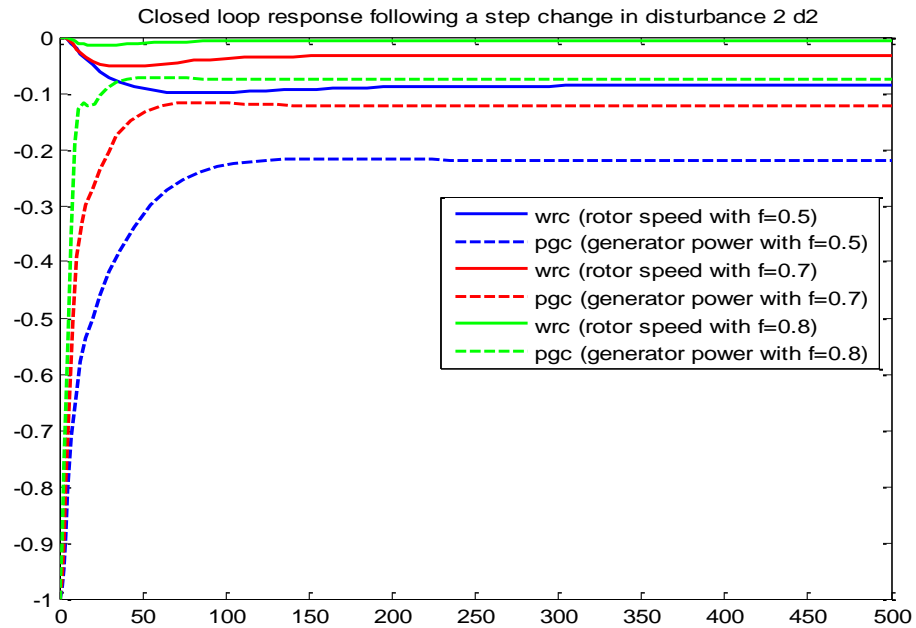


**Figure 4-10**, Closed Loop response following a step change in disturbance d2

The above figures depict that, how increasing the  $f_{1,2}$  from 0.5 to 0.8 improve the system output. Improvements are noticed in decreasing the rise time and the settling time. Also the non-interaction in the system outputs is achieved. The controller succeeds in suppressing the system disturbances reaching almost 100% recovery.

### Third order system with one zero:

It is interesting to analyze the response of the second output (the generated power) since it is under an effect of a third order system with one zero. Precisely, it is a sum of two transfer functions of linear system but one of them has a zero. Since the two transfer functions are of linear property, the rule of additivity is satisfied by the system of the second output. Because of that, the third order transfer function of one zero will be studied in the following lines.

$g_{21} = \frac{230.53s+11.54}{(s+0.016)(s^2+0.5s+0.075)}$  has a real pole  $s = -0.016$  and two complex conjugate poles at  $s = -0.251457 \pm 0.11484i$  in addition to one zero at  $s = -0.05$ .

The following Figure 4-11 shows the pole-zero plot of  $g_{21}$ . The dominant loop of the  $g_{21}$  is -0.016 because it is lying closer to the imaginary axis and has a persistence effect than the other far from the imaginary axis. The transient response component of the real pole can be written as an exponential function  $Ce^{-0.016t}$  and the complex conjugate poles can be written as  $Ce^{-0.25t}\cos(0.11t + \phi)$ .

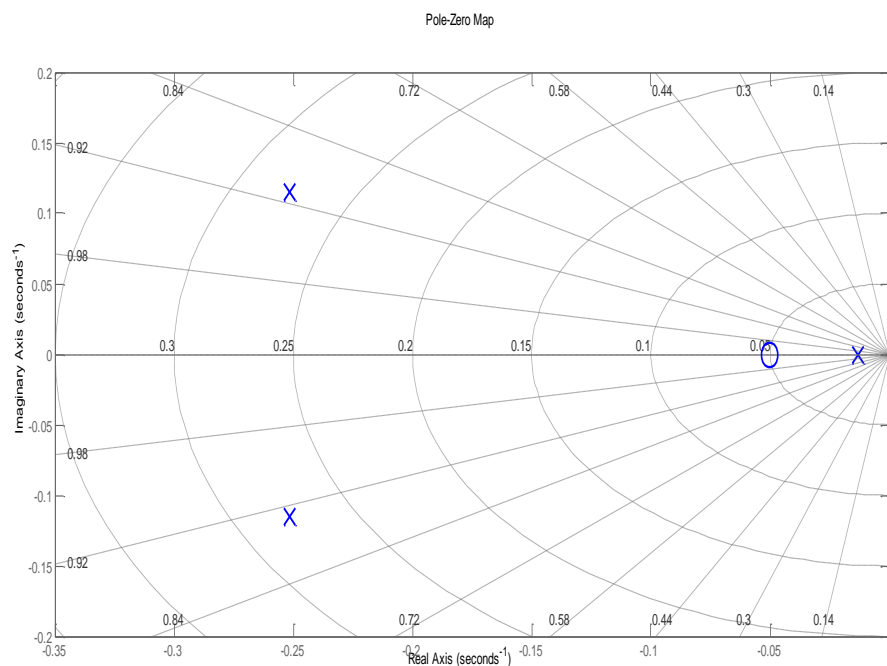


**Figure 4-11**, Pole-Zero graph of  $G_{21}$

After closing the loop for an arbitrary gain values of a proportional control  $K$ , the following Figure 4-12 shows the pole-zero plot of different proportional controller gains. Increasing the  $K$  yields to increasing in the imaginary part of the conjugate poles, that part is responsible for the oscillation in the transients when the value of  $f$  and  $P$  was being increased gradually.

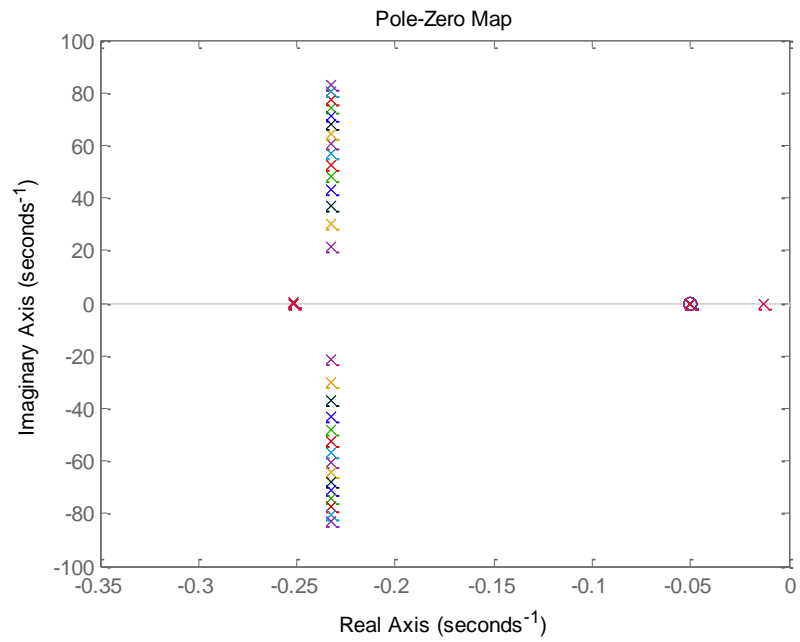


**Figure 4-12**, Pole-Zero graph for G21 for many proportional gain values

If the g21 zero is assumed to be not exist, the system would be unstable due to the increasing of the gain. But the zero existence helped in maintain the stability of the g21 function. Figure 4-13 depicts the previous assumption.

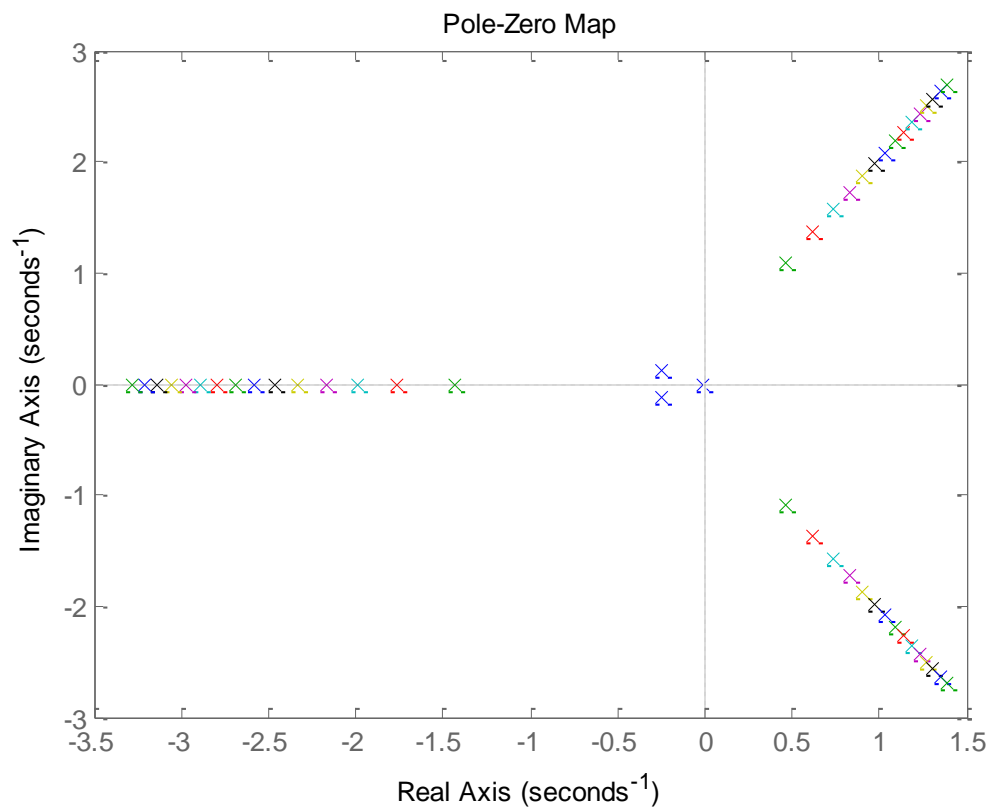


**Figure 4-13**, Pole-Zero graph of G21 with neglecting the zero

## 4.2.H-infinity Method.

The mixed sensitivity problem is to find a controller  $K$  that satisfies

$$\| [G_{11} + G_{12}K(I - G_{22}K)^{-1}G_{21}] \|_{\infty} \leq 1.$$

In other words, by choosing the proper weighting functions  $W_1, W_2$  and  $W_3$  a robust controller can be achieved.  $G(s), W_1, W_2$  and  $W_3$  are all proper, they are bounded as  $s \rightarrow \infty$ .

Since  $W_1$  is responsible to limit the error signal and as one typically wants to track only in the low frequencies,  $W_1$  is chosen as a low pass filter and to be small in the low frequencies region as the following matrix:

$$W_1 = \begin{bmatrix} \frac{10s + 100}{50s + 0.1} & 0 \\ 0 & \frac{10s + 100}{50s + 0.1} \end{bmatrix}$$

As  $W_1S \approx 1$ , therefore  $S$  will track inverse of  $W_1$ .

On the other hand, since noise typically occurs in high frequencies region so the  $W_2$  weighting function is chosen as:

$$W_2 = \begin{bmatrix} 10^{-5} & 0 \\ 0 & 10^{-5} \end{bmatrix}$$

$W_3$  filter is responsible to maintain the stability of the system, and it is needed to be small in the high frequencies:

$$W_3 = \begin{bmatrix} \frac{s + 1500}{s + 100} & 0 \\ 0 & \frac{s + 1500}{s + 10} \end{bmatrix}$$

By using the MATLAB function **mixsyn**, the controller functions are the following:

From input 1 to output 1 is  $K_{11}(s)=$

$$\frac{-2.558e-06 s^7 - 0.0004771s^6 - 0.03119s^5 - 231.5s^4 - 3.725e05s^3 - 3.495e07s^2 - 6.127e05s - 1086}{s^8 + 1701s^7 + 2.921e05s^6 + 1.871e07s^5 + 6.693e08s^4 + 1.2e10s^3 + 1.896e09s^2 + 7.441e06s + 7393}$$

From input 1 to output 2 is  $K_{21}(s) =$

$$\frac{-1.98e05s^7 - 3.202e08s^6 - 3.021e10 s^5 - 1.708e10s^4 - 3.293e09s^3 - 1.658e08 s^2 - 2.072e06s - 3507}{s^8 + 1701 s^7 + 2.921e05s^6 + 1.871e07s^5 + 6.693e08s^4 + 1.2e10s^3 + 1.896e09s^2 + 7.441e06s + 7393}$$

From input 2 to output 1 is  $K_{12}(s) =$

$$\frac{0.0001735s^8 + 0.09092s^7 + 13.53s^6 + 890.3s^5 + 3.391e04s^4 + 7.136e05s^3 + 4.497e06s^2 + 7.865e04s + 139.3}{s^8 + 1701s^7 + 2.921e05s^6 + 1.871e07s^5 + 6.693e08s^4 + 1.2e10s^3 + 1.896e09s^2 + 7.441e06s + 7393}$$

From input 2 to output 2 is  $K_{22}(s) =$

$$\frac{-403.4 s^7 - 6.369e05s^6 - 6.445e07s^5 - 4.389e08s^4 - 2.153e08 s^3 - 3.403e07s^2 - 5.404e05s - 946.4}{s^8 + 1701s^7 + 2.921e05s^6 + 1.871e07s^5 + 6.693e08s^4 + 1.2e10s^3 + 1.896e09s^2 + 7.441e06s + 7393}$$

By using the SIMULINK model of Figure 0-2 and applying the controller obtained by the H-infinity method, and with a step change in reference input  $I_f$  the following closed loop response is displayed in the following Figure 4-14:

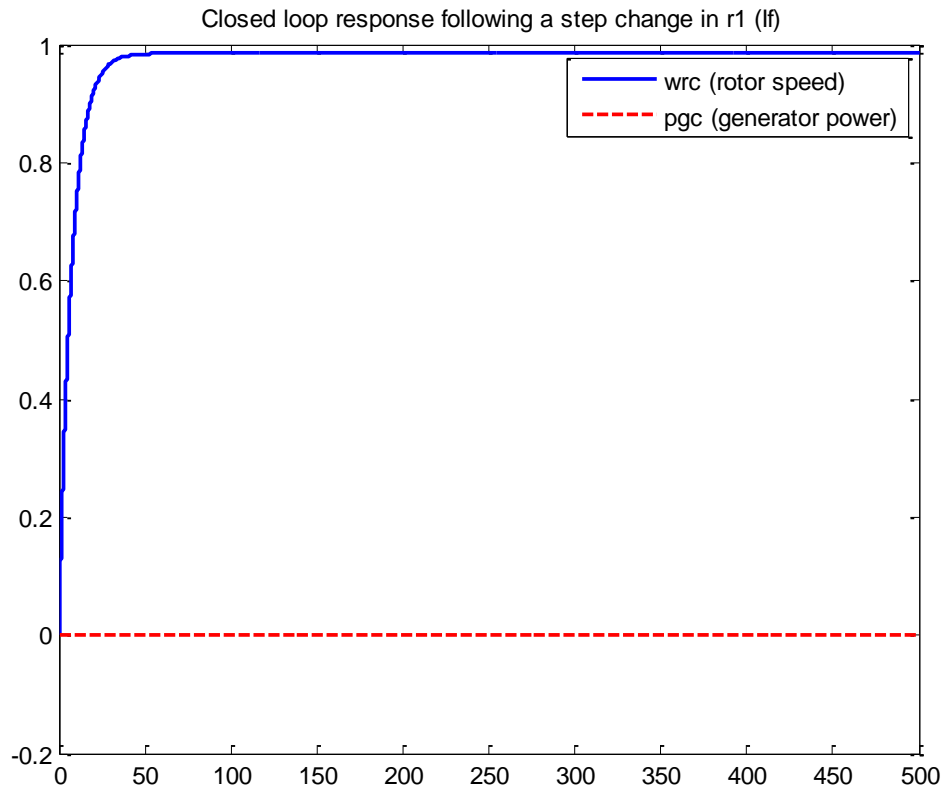


**Figure 4-14,** Closed loop response following a step change in  $r_1$  (If)

Moreover, when a step change in reference input  $B_{ref}$  is applied, the response will be as depicted in Figure 4-15 which shows fast response of settling time less than 100 seconds:

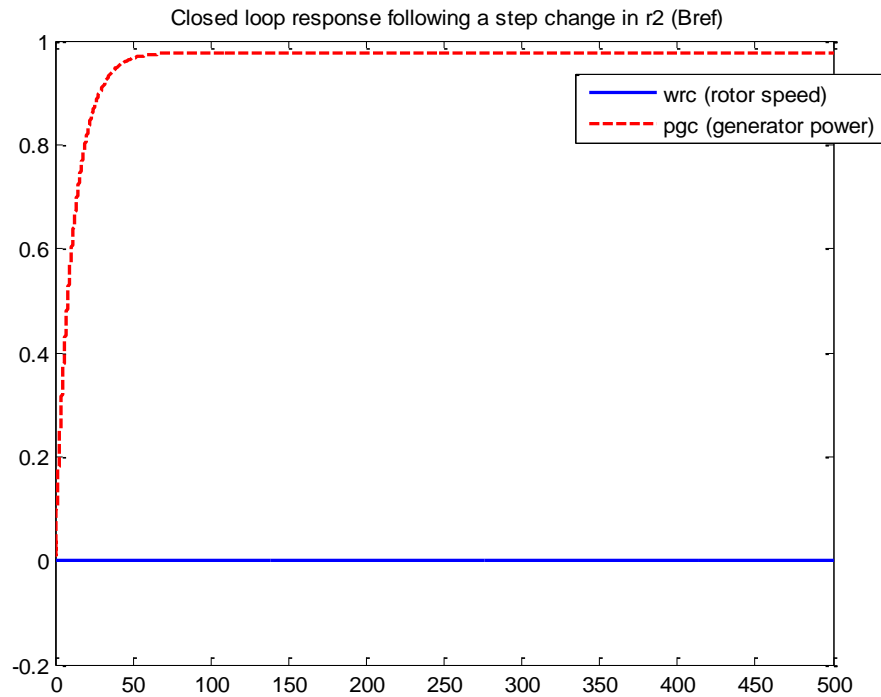


**Figure 4-15**, Closed loop response following a step change in r2 (Bref)

Besides that, and to check the robustness of the controller, a disturbance represented by a step change is applied on output 1 (rotor speed) and as shown in the Figure 4-16 an effective disturbance rejection is noticed and the controller act a quick recovery on the output.

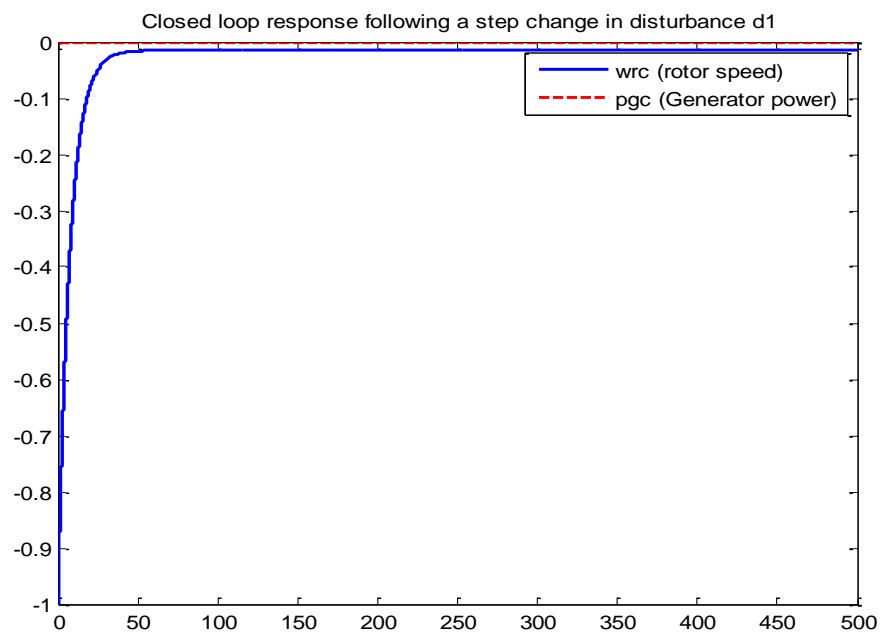


**Figure 4-16**, Closed loop response following a step change in disturbance d1

Along with that, and by applying a disturbance on the second output, the same fast recovery is remarked too, Figure 4-17.

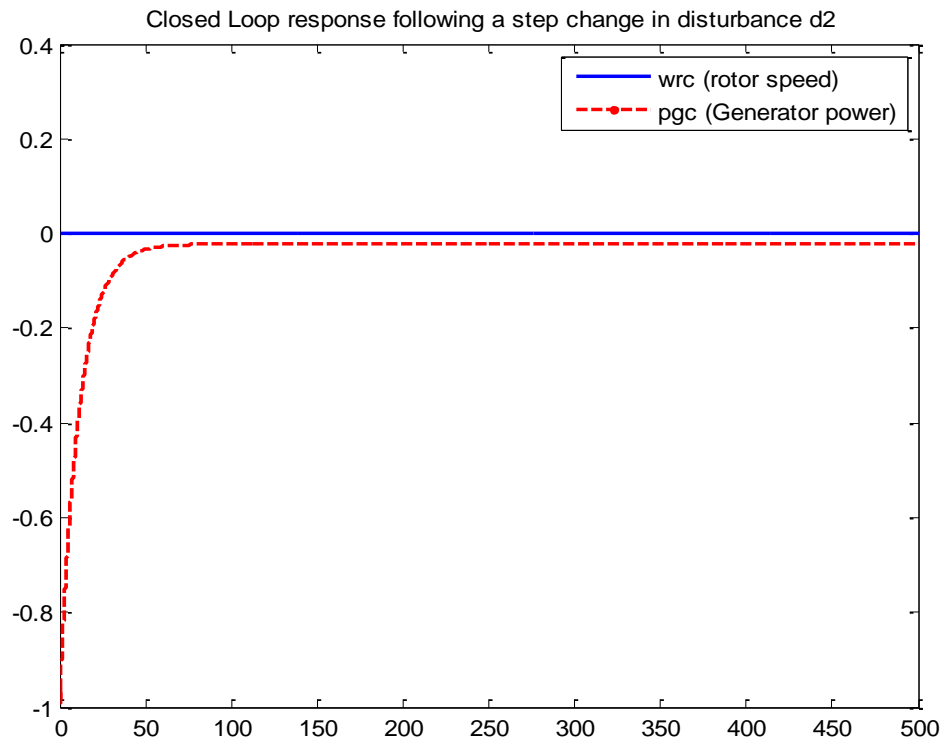


**Figure 4-17**, Closed loop response following a step change in disturbance d2

On the other hand, and for robustness confirmation, the following Figure 4-18 shows the singular values of the sensitivity functions.

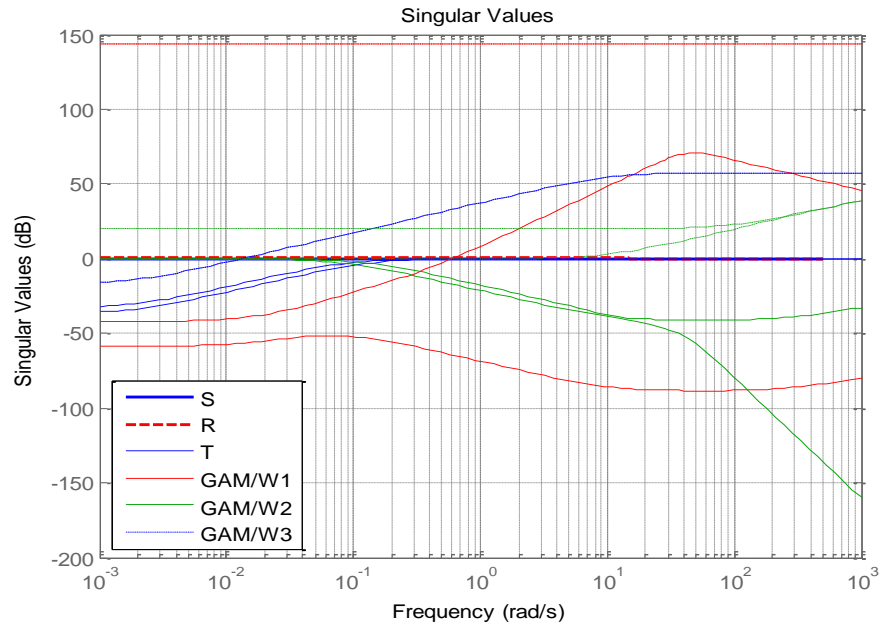


**Figure 4-18**, Singular values of sensitivity functions

Although of that, the system shows non-minimum phase in  $K_{11}(s)$  if the controller matrices are extracted into poles and zeros:

$$K_{11}(s) = \frac{-2.558e-06 (s+100) (s+0.01553) (s+0.002) (s^2 + 903.8s + 3.374e05) (s^2 - 817.4s + 4.049e05)}{(s+1516) (s+99.69) (s+44.43) (s+0.1553) (s+0.002)^2 (s^2 + 40.4s + 1772)}$$

$$K_{12}(s) = \frac{0.00017351 (s+329.3) (s+99.69) (s+44.6) (s+9.921) (s+0.01553) (s+0.002) (s^2 + 40.41s + 1779)}{(s+1516) (s+99.69) (s+44.43) (s+0.1553) (s+0.002)^2 (s^2 + 40.4s + 1772)}$$

$$K_{21}(s) = \frac{-1.9802e05 (s+1516) (s+100) (s+0.05006) (s+0.01558) (s+0.002) (s^2 + 0.5001s + 0.07487)}{(s+1516) (s+99.69) (s+44.43) (s+0.1553) (s+0.002)^2 (s^2 + 40.4s + 1772)}$$

$$K_{22}(s) = \frac{-403.41 (s+1471) (s+100.8) (s+6.781) (s+0.01558) (s+0.002) (s^2 + 0.5001s + 0.07487)}{(s+1516) (s+99.69) (s+44.43) (s+0.1553) (s+0.002)^2 (s^2 + 40.4s + 1772)}$$

### 4.3. Comparison Study.

The previous two sections show different results for the two designed controllers, and each technique has its advantages and disadvantages. For that, it is necessary to clarify and show the tradeoffs between the two methodologies. The comparison will be based on the application of both strategies in the real life problems, the closed loop response following a unit step input showing also the disturbance rejection of both controllers and at the end displays the difference in energy consumed by each controllers.

Least Effort is a methodology which takes place in the Laplace domain. It is necessary to have the transfer function of a form presented in section 3.3, so the transfer function needs to be manipulated without changing its dynamics by approximations. Approximation is not always sufficient for that, so pre-compensator needs to be employed for that purpose.

On the other hand, the H-infinity controller design procedure goes through two steps. The first is to find the weighting functions which describe the desired response and disturbance recovery of the plant in frequency domain. Secondly, the controller is designed for the “Loop shape”.

In result, the Least Effort controller has the simplest form where the feedback and feedforward are simple gains. Only the used pre-compensator added little complexity to the system. In contrast, the H-infinity controller has very complicated form where it is clear in the 8<sup>th</sup> order transfer functions matrices. Moreover, the H-infinity controller has non-minimum phase if

the poles and zeros forms are extracted. Which could affect the stability of the controller and make it fragile. Which makes the least effort controller a good choice in real applications.

It is necessary also to show how superior the two controllers are in disturbance rejection as shown in the figures of the simulation section. At the time the Least Effort controller provide almost 100% of disturbance rejected, the H-infinity disturbance rejection reaches 100% for both outputs. Moreover, it is clearly displayed that, the H-infinity controller has faster response and less overshooting with respect to the Least Effort controller.

However, in energy dissipation wise, the Least Effort controller is superior of the H-infinity. By applying a white noise and using the following formula (R. Whalley and M. Ebrahimi, 2006):

$$E(t) = \int_{t=0}^{t=1} (u_1(t)^2 + u_2(t)^2). dt$$

For 100 seconds, it can be seen from Figure 4-19, how the H-infinity controller consumes huge amount of energy appearing from multiplication by  $10^8$ . Meantime, the Least Effort controller consumes extremely low energy as depicted in the below figure.

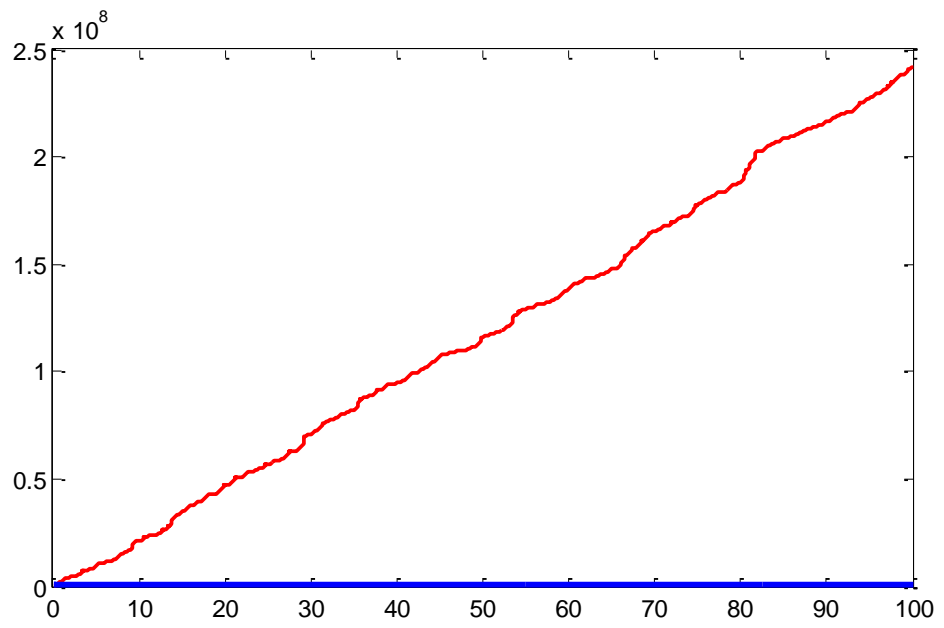


**Figure 4-19**, Energy Consumption by both controllers.

## Chapter V:

### 5. Conclusions and Recommendations

#### 5.1. Conclusions

This research was focused on applying two types of controllers. The Least Effort and H-infinity mixed sensitivity controllers, for VSWT. MATLAB and SIMULINK tools were used to compute, simulate, analyze and verify the controllers.

The Least effort controller, inner loop and outer loop were designed where it to help in maintain the stability and disturbance rejection characteristics, respectively. The optimization of the performance index was aimed at lowering the energy dissipation of the controller.

Alternatively, the careful selection of the weighting functions, for the desired K controller of the H-infinity was designed to achieve the maximum disturbance [MA1]rejection.

The Least Effort controller, met all the objectives of the research. Moreover, it displayed how with feedback and feedforward gains the controller can have significant disturbance recovery and noticeable decoupling of the plant's inputs and outputs.

Furthermore, the Least Effort controller has extremely low energy consumption which draws the attention of any designer in the renewable energy industry where the energy consumption is important.

On the other hand, H-infinity controller response is very fast and of smooth output. But, because of the complexity of the controller design and high energy consumption makes it unfavourable in the renewable energy industry. The wind turbine could not respond in reality to the controller where the acceleration forces would cause mechanical damages.

## 5.2.Recommendations:

The Least Effort controller is recommended for multivariable systems and in the fields where the energy consumption is paramount. Moreover, The Least Effort controller can be extended and used on other Wind Turbine and similar large systems.

In contrast, simplifying the  $K(s)$  controller of H-infinity method would have to be achieved for practicality reasons. However, in simplifying the closed loop  $K(s)$ , stability cannot ever be guaranteed and in therefore not feasible.

### 5.3.References

González, M., Garrido, J., Morilla, F. & Vázquez, F. (2011). Multivariable Centralized Control with Decoupling and Feedforward Compensation for Residential Wind Turbine. *IFAC Proceedings Volumes*, vol. 44 (1), pp. 557-562.

Owens, D. (2002). A HISTORICAL VIEW OF MULTIVARIABLE FREQUENCY DOMAIN CONTROL. *IFAC Proceedings Volumes*, vol. 35 (1), pp. 225-230.

Leigh, J. (2012). *Control Theory a guided tour*. 3rd edn. London: The Institution of Engineering and Technology.

National Renewable Energy Laboratory. (2001). *The History and State of the Art of Variable-Speed Wind Turbine Technology* [online]. Colorado: National Renewable Energy Laboratory. [Accessed 6 October 2017]. Available at: <https://www.nrel.gov/docs/fy01osti/28607.Pdf>

Hoffmann, R. (2002). *A comparison of control concepts for wind turbines in terms of energy capture*. Dipl.-Ing. Technischen Universität Darmstadt.

Martinez, J. (2007). *Modelling and Control of Wind Turbines*. Master of Science in Process Systems Engineering. Imperial College London.

"Wind Turbine Control Methods - National Instruments". (2016). [Accessed 18 October 2016].

Available at: <http://www.ni.com/white-paper/8189/en/>

*Wind Power Technology Brief*. (2016). 1st edn. IEA-ETSAP and IRENA. Viewed 18 October 2016. <http://www.irena.org/Publications>

"How a Wind Turbine Works". (2016). [Accessed 22 October 2016]. Available at:

<http://www.energy.gov/articles/how-wind-turbine-works>

Treurnicht, J. (2007). *H $\infty$  Control*. 1st edn. Viewed 15 April 2017.

[http://courses.ee.sun.ac.za/Robuuste\\_Beheerstelsels\\_813/images/hinf2007.pdf](http://courses.ee.sun.ac.za/Robuuste_Beheerstelsels_813/images/hinf2007.pdf)

Maciejowski, J. (1996). *Multivariable feedback design*. 1st edn. Wokingham [u.a.]: Addison-Wesley.

McFarlane, D. & Glover, K. (1992). A loop-shaping design procedure using H/sub infinity / synthesis. *IEEE Transactions on Automatic Control*, vol. 37 (6), pp. 759-769.

Nof, S. (2009). *Springer handbook of automation*. 1st edn. Berlin [u.a.]: Springer.

Bennett, S. (1986). *A history of control engineering*. 1st edn. London, U.K.:P. Peregrinus.

Zames, G. (1976). Feedback and complexity, Special plenary lecture addendum. *IEEE Conf. Decision Control*. IEEE Conf. Decision Control. [Accessed 29 May 2017].

Zames, G. (1981). Feedback and optimal sensitivity: Model reference transformations, multiplicative seminorms, and approximate inverses. *IEEE Transactions on Automatic Control*, vol. 26 (2), pp. 301-320.

"10 big wind turbines | Windpower Monthly". (2017). [Accessed 4 June 2017]. Available at: <http://www.windpowermonthly.com/10-biggest-turbines>

National Renewable Energy Laboratory. (2001). *the History and State of the Art of Variable-Speed Wind Turbine Technology*. Golden, Colorado 80401-3393:U.S. Department of Energy and its contractors. [Accessed 6 June 2017].

Polinder, H., de Haan, S., Dubois, M. & (Han) Slootweg, J. (2005). Basic Operation Principles and Electrical Conversion Systems of Wind Turbines. *EPE Journal*, vol. 15 (4), pp. 43-50.

Polinder, H., Slootweg, J. & Kling, W. (2001). Dynamic modeling of a wind turbine with direct drive synchronous generator and back to back voltage source converter. *European Wind Energy Conference* [online]. Copenhagen. Copenhagen. [Accessed 8 June 2017]. Available at: [https://www.researchgate.net/publication/262642598\\_Dynamic\\_modeling\\_of\\_a\\_wind\\_turbine\\_w](https://www.researchgate.net/publication/262642598_Dynamic_modeling_of_a_wind_turbine_w)

ith direct drive synchronous generator and back to back voltage source converter and its control

"The Wind Energy Pioneer - Poul la Cour". (n.d.). [Accessed 8 June 2017]. Available at:  
<http://xn--drmstrre-64ad.dk/wp-content/wind/miller/windpower%20web/en/pictures/lacour.htm>

Muller, S., Deicke, M. & De Doncker, R. (2002). Doubly Fed Induction Generator Systems. *IEEE Industry Applications Magazine*.

Whalley, R. & Ebrahimi, M. (2006). Multivariable System Regulation. *Proceedings of the Institution of Mechanical Engineers, Part C: Journal of Mechanical Engineering Science*, vol. 220 (5), pp. 653-667. [Accessed 10 July 2017].

Whalley, R., El-Shalabi, S., Ebrahimi, M. & Abdul-Ameer, A. (2009). Adaptive machine tool system regulation. *IET Control Theory & Applications*, vol. 3 (1), pp. 33-48. [Accessed 10 July 2017].

Blackwood, M. (2016). Maximum Efficiency of a Wind Turbine. *Undergraduate Journal of Mathematical Modeling: One + Two*, vol. 6 (2).

Akbarzadeh, A. (1992). *Fundamentals of remote area power supply systems*. Melbourne: Renewable Energy Authority of Victoria (Energy Victoria).

Verma, M. & Jonckheere, E. (1984).  $L_\infty$ -compensation with mixed sensitivity as a broad-band matching problem. *Systems & Control Letters* [online]. Vol. 4 (3), pp. 125-129. [Accessed 20 September 2017]. Available at:

<http://www.sciencedirect.com/science/article/pii/S0167691184800134?via%3Dihub>

Bansal A. and Sharma V.,( 2013), *Design and Analysis of Robust H-infinity Controller*, National Conference on Emerging Trends in Electrical, Instrumentation & Communication Engineering, Vol.3, No.2, 2013

Myr, O. (1970). *The Origins of Feedback Control*. 1st edn. Massachusetts: The MIT press.

Tolaimate, I. & Elalami, N. (2011). Robust Control Problem as  $H_2$  and  $H_\infty$  control problem applied to the robust controller design of Active Queue Management routers for Internet Protocol. *INTERNATIONAL JOURNAL OF SYSTEMS APPLICATIONS, ENGINEERING & DEVELOPMENT*, vol. 6 (5). [Accessed 2 October 2017].

Dingyu X, YangQuan C and Derek P, (2007), *Linear Feedback Control Analysis and Design with MATLAB*, Siam, Philadelphia, 2007.

Bergbreiter,S.(2005). *Moving From Practice to Theory: Automatic Control after World War II*. [Online]. [Accessed 06 October 2017]. Available at:

<https://www.scribd.com/document/42081943/Moving-From-Practice-to-Theory-Automatic-Control-After-World-War-II-BergbreiterHIS285S>

Dorf, R.C. and Bishop, R.H. (2008). *Modern Control Systems*. Pearson Education, Inc.

Gopal M., (2008), *Control Systems: Principles and Design*, Tata McGraw-Hill Publishing Company Limited, New Delhi.

Megdadi, E. (2017). *A Comparative Design Study for Gas Turbine Regulation using Least Effort Control*. MSc. The British University in Dubai.

El-Hassan, T. (2012). *A Design Study for Multivariable Feedback Control System Regulation for Aircraft Turbo-Jet Engines*. MSc. The British University in Dubai.

Bansal, A. & Sharma, V. (2013). Design and Analysis of Robust H-infinity Controller. *Control Theory and Informatics*. National Conference on Emerging Trends in Electrical, Instrumentation & Communication Engineering. National Institute of Technology: Hamirpur, India.

Bibel, J. & Malyevac, D. (1992). Guidelines for the Selection of Weighting Functions for H-INFINITY Control. *Naval Surface Warfare Center Dahlgren Division*, (NSWCDD/MP-92/43).

H.Bosgra, O., Kwakernaak, H. & Meinsma, G. (2008). *Design Methods for Control Systems*. Enschede: Dutch Institute of Systems and Control. Viewed 30 May 2017.

<http://wwwhome.math.utwente.nl/~meinsmag/dmcs/dmcs0708.pdf>

Dukkipati, R. (2006). *Analysis and design of control systems using MATLAB*. New Delhi: New Age International (P) Limited, Publishers.

Xue, D., Chen, Y. & Atherton, D. (2007). *Linear feedback control*. Philadelphia: Society for Industrial and Applied Mathematics.

Chiang, R. & Safonov, M. (2006). *Robust Control Toolbox for use with MATLAB®*. Natick, Mass.:MathWorks.

## Appendix

**SIMULINK model:**

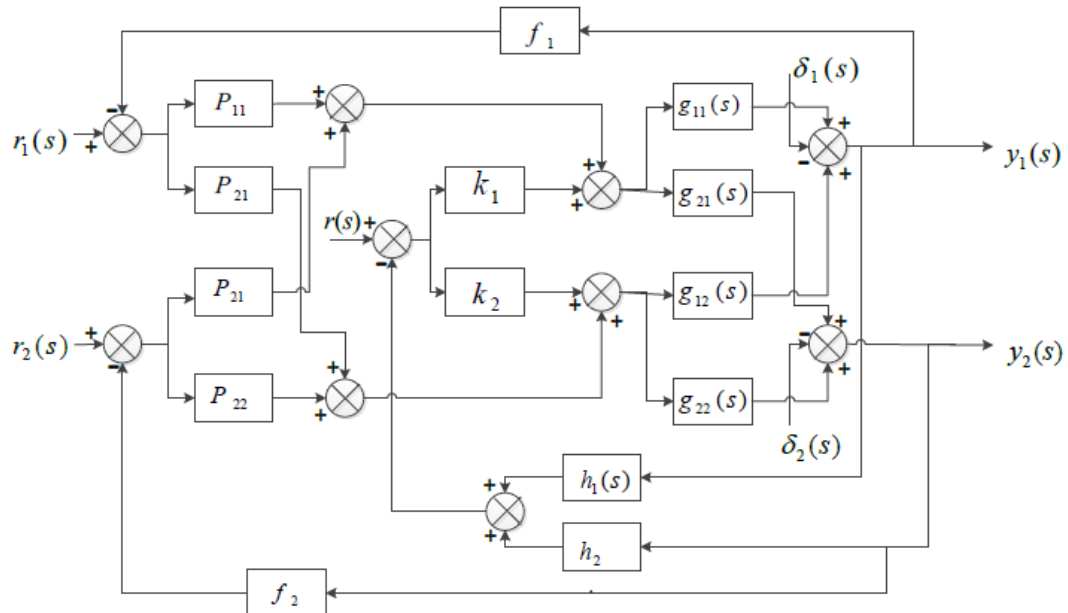


**Figure A-1**, Least Effort Controller Simulation Model (Megdadi 2017)

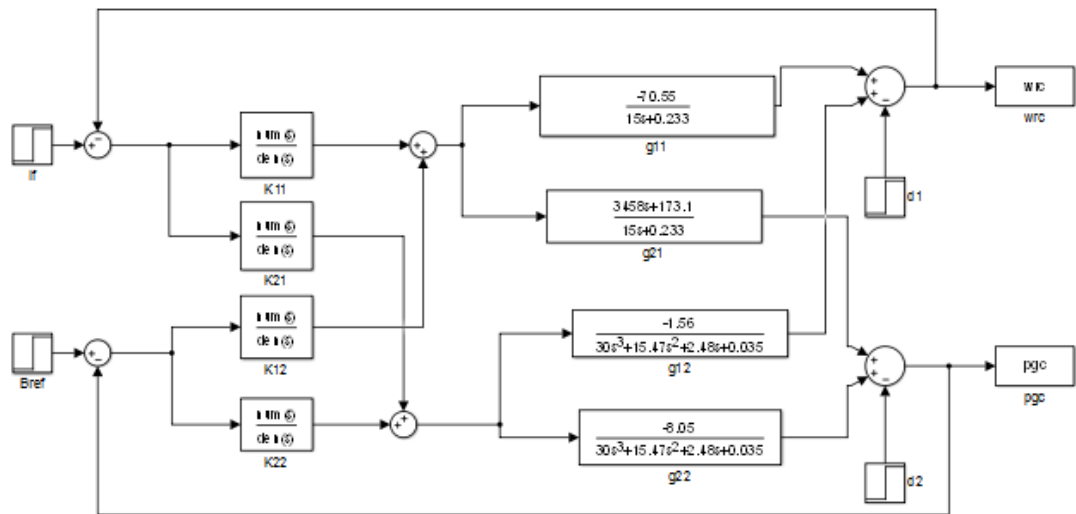


**Figure 0-2,** H-infinity controller Simulation model.

## MATLAB code:

- **Least Effort Control**

```
clear all

clc

format short

%inner loop design

syms n s

Q=[-4.7-0.0520*n, 11.53-0.268*n; 0, 230.53];

Qi=inv(Q);

Qit=transpose(Qi);

b0=0.013;

b=b0*[0.016;1];

bs=b0*(s+0.016);

bt=transpose(b);

%ds=(s+0.016)*((s^2+0.5*s+0.075));

rlc=tf([b0],[1 0.5 0.075]);%b(s)/d(s) single transfer function equivalent to
the closed loop multivariable system

%rlocus(rlc)

j=(1+n^2)*bt*Qit*Qi*b;

jmin=diff(j);

x=solve(jmin);% finding the roots of jmin which is derivative of j

y=subs(j,n,x);% substituting the roots in j and find the root which gives min
index

z=subs(Qi,n,0.033319784275263475940091363415985); % substituting the root in
the inverse of Q where 0.033 is the n when j is min.

h=vpa(z*b);

%Outer loop design

Gs=[-4.7/(s^3+0.516*s^2+0.083*s+0.001), -
0.0520/(s^3+0.516*s^2+0.083*s+0.001);
```

```

(230.5*s+11.54)/(s^3+0.516*s^2+0.083*s+0.001), -
0.2683/(s^3+0.516*s^2+0.083*s+0.001)]
G0=subs(Gs,0);
G0i=inv(G0);
Ss=[1,0.1;0.1,1];
I2=[1,0;0,1];
k=[1 ;0.033319784275263475940091363415985];
f=[0.8,0;0,0.8];
ht=transpose(h);
%P=(G0i+(k*ht))*Ss*inv(I2-f*Ss)
P=(G0i+k*ht)*Ss*inv((I2-f*Ss));
Pdouble=double(P);
hd=double(h);

```

### **H-infinity Code:**

```

clear all
clc
format shorteng
G=[tf([-70.55],[15 0.233]) tf([-1.56],[30 15.47 2.48 0.035]); tf([3458
173.1],[15 0.233]) tf([-8.05],[30 15.47 2.48 0.035])]
sys=ss(G,'min'); % to find the state space matrices in its minimum
realization.
A=[-0.01553 0 0 0; 0 -0.5157 -0.3307 -0.07467; 0 0.25 0 0; 0 0 0.0625 0];
B=[4 0; 0 4; 0 0; 0 0];% found from the above
C=[-1.176 0 0 -0.832; 1.99 0 0 -4.293];
D=[0 0; 230.5 0];
s=tf('s');

```

```

W1=[(10*s+100)/(50*s+0.1),0; 0,(10*s+100)/(50*s+0.1)];

W2 = [tf(1e-5),0; 0,tf(1e-5)];

%W3 = [(s+1500)/((0.1*s+1500)),0;0,(s+1500)/(0.1*s+1500)];

W3 = [(s+1500)/((s+100)),0;0,(s+1500)/(s+10)];

[K,CL,GAM] = mixsyn(G,W1,W2,W3);% controller

Ktf=tf(K);

P = augw (G, W1, W2, W3);% Extended Plant:

Gc=Ktf;

[numk11,denk11] = tfdata(Ktf(1,1));

[numk21,denk21] = tfdata(Ktf(2,1));

[numk12,denk12] = tfdata(Ktf(1,2));

[numk22,denk22] = tfdata(Ktf(2,2));

set_param('closed_loop_Hinf/K11','Numerator','numk11{1}','Denominator','denk11{1}');

set_param('closed_loop_Hinf/K21','Numerator','numk21{1}','Denominator','denk21{1}');

set_param('closed_loop_Hinf/K12','Numerator','numk12{1}','Denominator','denk12{1}');

set_param('closed_loop_Hinf/K22','Numerator','numk22{1}','Denominator','denk22{1}');

N = lft (P, K);% Entire System:

L = G * K; % Open Loop:

S = feedback(eye(2),L);%sensitivity function

R=K*S; %control effort

T = eye(2)-S;% Closed Loop (complementary sensitivity function

%Hinf=norm(plant,inf)

```

```
sigma(S, 'b', R, 'r', T, 'g', GAM/W1, 'b-', ss(GAM/W2), 'r-', GAM/W3, 'g-', {1e-  
3, 1e3});  
legend('S', 'R', 'T', 'GAM/W1', 'GAM/W2', 'GAM/W3', 'Location', 'SouthWest');  
grid;  
K11=zpk(K(1,1))  
K12=zpk(K(1,2))  
K21=zpk(K(2,1))  
K22=zpk(K(2,2))
```